

 Open access • Journal Article • DOI:10.1136/GUTJNL-2020-321565

## **Microbiota tryptophan metabolism induces aryl hydrocarbon receptor activation and improves alcohol-induced liver injury. — Source link**

Laura Wrzosek, Dragos Ciocan, Cindy Hugot, Madeleine Spatz ...+16 more authors





**Institutions:** Université Paris-Saclay, French Institute of Health and Medical Research, Institut Gustave Roussy, University of Paris

**Published on:** 01 Jul 2021 - Gut (BMJ Publishing Group)

**Topics:** Alcoholic liver disease, Aryl hydrocarbon receptor, Alcoholic hepatitis, Liver injury and Metabolome

Related papers:

- [Aryl Hydrocarbon Receptor Deficiency in Intestinal Epithelial Cells Aggravates Alcohol-Related Liver Disease.](#)
- [Intestinal microbiota-derived tryptophan metabolites are predictive of Ah receptor activity](#)
- [Activation of AhR-NQO1 Signaling Pathway Protects Against Alcohol-Induced Liver Injury by Improving Redox Balance](#)
- [Polyphenols and Tryptophan Metabolites Activate the Aryl Hydrocarbon Receptor in an in vitro Model of Colonic Fermentation.](#)
- [Aryl Hydrocarbon Receptor Activity in Hepatocytes Sensitizes to Hyperacute Acetaminophen-Induced Hepatotoxicity in Mice.](#)

Share this paper:    

View more about this paper here: <https://typeset.io/papers/microbiota-tryptophan-metabolism-induces-aryl-hydrocarbon-16zbvnsjdp>



**HAL**  
open science

## **Microbiota tryptophan metabolism induces aryl hydrocarbon receptor activation and improves alcohol-induced liver injury**

Laura Wrzosek, Dragos Ciocan, Cindy Hugot, Madeleine Spatz, Margot Dupeux, Camille Houron, Vanessa Liévin-Le Moal, Virginie Puchois, Gladys Ferrere, Nicolas Trainel, et al.

### ► To cite this version:

Laura Wrzosek, Dragos Ciocan, Cindy Hugot, Madeleine Spatz, Margot Dupeux, et al.. Microbiota tryptophan metabolism induces aryl hydrocarbon receptor activation and improves alcohol-induced liver injury. *Gut*, BMJ Publishing Group, 2021, 70 (7), pp.1299-1308. 10.1136/gutjnl-2020-321565 . hal-03329872

**HAL Id: hal-03329872**

**<https://hal.sorbonne-universite.fr/hal-03329872>**

Submitted on 31 Aug 2021

**HAL** is a multi-disciplinary open access archive for the deposit and dissemination of scientific research documents, whether they are published or not. The documents may come from teaching and research institutions in France or abroad, or from public or private research centers.

L'archive ouverte pluridisciplinaire **HAL**, est destinée au dépôt et à la diffusion de documents scientifiques de niveau recherche, publiés ou non, émanant des établissements d'enseignement et de recherche français ou étrangers, des laboratoires publics ou privés.

1 **Microbiota tryptophan metabolism induces aryl hydrocarbon receptor activation and**  
2 **improves alcohol-induced liver injury**

3 Laura Wrzosek<sup>1,2§</sup>, Dragos Ciocan<sup>1,2,3§</sup>, Cindy Hugot<sup>1,2</sup>, Madeleine Spatz<sup>1,2</sup>, Margot Dupeux<sup>1,2,4</sup>,  
4 Camille Houron<sup>1,2</sup>, Vanessa Liévin-Le Moal<sup>1,2</sup>, Virginie Puchois<sup>1,2</sup>, Gladys Ferrere<sup>1,2</sup>, Nicolas  
5 Trainel<sup>1,2</sup>, Françoise Mercier-Nomé<sup>5</sup>, Sylvère Durand<sup>6</sup>, Guido Kroemer<sup>7</sup>, Cosmin Sebastian  
6 Voican<sup>1,2,3</sup>, Patrick Emond<sup>8,9</sup>, Marjolene Straube<sup>10</sup>, Harry Sokol<sup>10,11,12</sup>, Gabriel Perlemuter<sup>1,2,3\*</sup>,  
7 and Anne-Marie Cassard<sup>1,2\*</sup>

8

9 <sup>§</sup>These authors contributed equally to the work.

10 \*Corresponding authors:

11 Anne-Marie Cassard : INSERM U996, 32 rue des carnets 92190 Clamart, France.

12 Tel: +33 1 41 28 80 37

13 Fax: +33 1 46 32 79 93

14 [cassard.doulicier@u-psud.fr](mailto:cassard.doulicier@u-psud.fr)

15 Gabriel Perlemuter : INSERM U996, 32 rue des carnets, 92190 Clamart, France.

16 Tel: +33 1 41 28 80 37

17 Fax: +33 1 46 32 79 93

18 [gabriel.perlemuter@aphp.fr](mailto:gabriel.perlemuter@aphp.fr).

19

20 <sup>1</sup>Université Paris-Saclay, Inserm U996, Inflammation, Microbiome and Immunosurveillance,  
21 92140, Clamart, France.

22 <sup>2</sup>Institut Paris-Sud d'Innovation Thérapeutique (IPSIT), IFR141, Faculté de Pharmacie, Univ  
23 Paris-Sud, Université Paris-Saclay, Châtenay-Malabry, France. <sup>3</sup>AP-HP, Hepato-  
24 Gastroenterology and Nutrition, Hôpital Antoine-Béclère, Clamart, France. <sup>4</sup>AP-HP,  
25 Anatomie-Pathologique, Hôpital Kremlin-Bicêtre, le Kremlin-Bicêtre, France. <sup>5</sup>Université  
26 Paris-Saclay, Inserm, CNRS, Institut Paris Saclay d'Innovation thérapeutique, 92296,  
27 Châtenay-Malabry, France. <sup>6</sup>Metabolomics and Cell Biology Platforms, Gustave Roussy  
28 Cancer Campus, Villejuif, France. <sup>7</sup>Gustave Roussy Cancer Campus, Villejuif, France;  
29 INSERM, U1138, Paris, France; Equipe 11 labellisée par la Ligue Nationale contre le Cancer,  
30 Centre de Recherche des Cordeliers, Paris, France; Université Paris Descartes/Paris V,  
31 Sorbonne Paris Cité, Paris, France; Metabolomics and Cell Biology Platforms, Gustave Roussy  
32 Cancer Campus, Villejuif, France; Université Pierre et Marie Curie, Paris, France; Pôle de  
33 Biologie, Hôpital Européen Georges Pompidou, AP-HP, Paris, France; Karolinska Institute,

1 Department of Women's and Children's Health, Karolinska University Hospital, Stockholm,  
2 Sweden. <sup>8</sup>UMR 1253, iBrain, Université de Tours, Inserm, Tours, France. <sup>9</sup>CHRU de Tours,  
3 Service de Médecine Nucléaire In Vitro, Tours, France. <sup>10</sup>Sorbonne Université, Inserm, Centre  
4 de Recherche Saint-Antoine, CRSA, AP-HP, Hôpital Saint Antoine, Service de  
5 Gastroenterologie, F-75012 Paris, France. <sup>11</sup>Gastroenterology Department, Saint-Antoine  
6 Hospital, Assistance Publique-Hôpitaux de Paris (AP-HP), Paris, France. <sup>12</sup>INRA, UMR1319  
7 Micalis, AgroParisTech, Jouy-en-Josas, France.

8

9 **Electronic word count: 4052**

10

11 **Number of figures and tables: 5 figures**

12

13

14 **Keywords:** alcoholic hepatitis, indole, fecal microbiota transplantation, human microbiota  
15 associated mice, fiber, pectin

1 **ABSTRACT**

2 **Objective:** Chronic alcohol consumption is an important cause of liver-related deaths. Specific  
3 intestinal microbiota profiles are associated with susceptibility or resistance to alcoholic liver  
4 disease in both mice and humans. We aimed to identify the mechanisms by which targeting  
5 intestinal microbiota can improve alcohol-induced liver lesions.

6 **Design:** We used human associated mice, a mouse model of alcoholic liver disease transplanted  
7 with the intestinal microbiota of alcoholic patients and used the prebiotic, pectin, to modulate  
8 the intestinal microbiota. Based on metabolomic analyses, we focused on microbiota tryptophan  
9 metabolites, which are ligands of the aryl hydrocarbon receptor (AhR). Involvement of the AhR  
10 pathway was assessed using both a pharmacological approach and AhR-deficient mice.

11 **Results:** Pectin treatment modified the microbiome and metabolome in human microbiota-  
12 associated alcohol-fed mice, leading to a specific fecal signature. High production of bacterial  
13 tryptophan metabolites was associated with an improvement of liver injury. The AhR agonist  
14 FICZ (6-formylindolo (3,2-b) carbazole) reduced liver lesions, similarly to prebiotic treatment.  
15 Conversely, inactivation of the *ahr* gene in alcohol-fed AhR *knock-out* mice abrogated the  
16 beneficial effects of the prebiotic. Importantly, patients with severe alcoholic hepatitis have low  
17 levels of bacterial tryptophan derivatives that are AhR agonists.

18 **Conclusions:** Improvement of alcoholic liver disease by targeting the intestinal microbiota  
19 involves the AhR pathway, which should be considered as a new therapeutic target.

1 **SUMMARY BOX**

2 **What is already known about this subject?**

- 3 • The intestinal microbiota is a causal factor of alcohol-induced liver lesions in mice and  
4 humans.  
5 • Pectin is able to prevent alcohol-induced liver injury in mice by altering the intestinal  
6 microbiota.  
7 • The protective effect of pectin is associated with an improvement of gut barrier function.  
8

9 **What are the new findings?**

- 10 • Moderate amount of pectin can cure alcoholic liver disease in the context of the human  
11 microbiota.  
12 • Pectin increases the production of tryptophan metabolites, which are aryl hydrocarbon  
13 receptor (AhR) ligands, by the microbiota, improving gut barrier function.  
14 • Pharmacological activation of the AhR by FICZ, an exogenous AhR ligand, is sufficient to  
15 simulate the effect of pectin.  
16 • AhR deficiency abrogates the beneficial effect of pectin, demonstrating a major role for the  
17 AhR pathway in the protective effect of the intestinal microbiota.  
18

19 **How might it impact on clinical practice in the foreseeable future?**

20 Therapeutic options in alcohol-induced liver injury are limited. Our results show that targeting  
21 intestinal microbiota using moderate amount of pectin can reverse alcohol-induced liver injury  
22 through the AhR pathway. Modifying intestinal microbiota to increase its production of AhR  
23 ligands or AhR ligand administration could be new therapeutic targets for alcoholic patients.

## 1 INTRODUCTION

2 Chronic alcohol consumption is a major cause of liver-related deaths [1]. Severe  
3 alcoholic hepatitis (sAH) is a life-threatening form of alcoholic liver disease (ALD), with few  
4 therapeutic options [2]. Recent studies have shown that specific microbiota profiles are  
5 associated with susceptibility or resistance to alcohol-induced liver lesions in both mice and  
6 humans, opening new therapeutic options [3, 4, 5, 6]. Moreover, the production of cytotoxin by  
7 *Enterococcus faecalis* has been specifically shown to be involved in ALD development in 30%  
8 of sAH patients and its eradication by phagotherapy improves liver injury in a mouse model of  
9 ALD [7, 8]. Aside from deleterious bacteria, it is also relevant to identify bacteria that can  
10 protect patients from developing alcohol-induced liver lesions and to understand the molecular  
11 mechanisms involved in such protective effects.

12 Several studies have reported that modulation of intestinal microbiota (IM) composition  
13 by fecal microbiota transfer [4, 5, 9] or treatment with *Akkermansia muciniphila* [10], *Roseburia*  
14 *intestinalis* [11], other probiotics, or fiber/prebiotics [12, 13] can improve liver injury in mouse  
15 models of ALD. Molecular mechanisms by which microbiota alterations can improve alcohol-  
16 induced liver lesions are poorly understood and involve changes in the gut barrier and bacterial  
17 metabolites.

18 Disruption of the gut barrier correlates with endotoxemia and the severity of ALD in  
19 humans and mice [4, 5, 14]. This disruption is associated with a decrease in the production of  
20 mucus and anti-microbial peptides and the disruption of tight junctions [15, 16, 17]. Modulation  
21 of the IM by fecal transfer, prebiotics, or probiotics restores a leaky gut [4, 6, 13, 15]. Moreover,  
22 changes in IM composition in patients with ALD induce modifications in microbiota-associated  
23 metabolites, including short chain fatty acids (SCFAs) and bile acids [12], and are involved in  
24 the severity of alcohol-induced liver injury [5, 18, 19]. Among microbiota-associated  
25 metabolites, tryptophan-derived indoles, produced by a large number of bacteria, including  
26 *Bacteroides*, are ligands of the aryl hydrocarbon receptor (AhR). AhR signaling improves the  
27 function of the intestinal barrier by increasing local expression of IL-22 [20, 21] and,  
28 consequently, increases expression of antimicrobial proteins [22]. Moreover, the abundance of  
29 Bacteroidetes and level of plasma tryptophan decrease after acute alcohol administration in  
30 humans, suggesting impaired tryptophan metabolism [23].

31 Here, we aimed to identify the mechanisms by which targeting the IM with a prebiotic can  
32 improve alcohol-induced liver lesions. We used human microbiota-associated mice (HMA),  
33 which were transplanted with the IM of patients with sAH, to work in the context of the human

1 microbiota. We used the prebiotic fiber, pectin, to alter the IM. We and others have already  
2 shown that pectin can modify the mouse IM and prevent ALD by improving the leaky gut-  
3 barrier. However, the molecular mechanisms involved in this process and the effects of pectin  
4 in the context of the human IM are still unknown [4, 6]. We now demonstrate that pectin  
5 reshapes the microbiome in the context of the human microbiota and not only prevents but also  
6 reverses alcohol-induced liver injury in mice. Metabolomic studies showed that changes in the  
7 microbiota composition also induced alterations in bacterial tryptophan metabolism, leading to  
8 the high production of indole derivatives, which activate the AhR. Pharmacological treatment  
9 of mice with an AhR agonist simulating the effect of pectin on the liver and reversed ALD,  
10 whereas inactivation of the *ahr* gene in knock-out mice abrogated the effects of the beneficial  
11 microbiota in alcohol-fed mice. The results observed in the humanized mice are also supported  
12 by a decreased level of AhR agonists in patients with sAH, suggesting that AhR may be a new  
13 therapeutic target in ALD.

14



## 1 MATERIAL AND METHODS

2 **Mice.** Female C57BL/6J mice (Janvier laboratory, Le Genest, France) were kept in humidity  
3 and temperature-controlled rooms, on a 12-hour light-dark cycle. Mice had access to a chow  
4 diet and water *ad libitum* before the study. Body weight and food intake were measured three  
5 times a week. All our experimental procedures were validated by the ethical committees and  
6 the French veterinary minister (2015052715405651\_v2 (APAFIS#729) and  
7 2017042314557080v1(APAFIS#4788).

8  
9 **Treatments.** In all our experiments, pectin was given at D21, as a curative treatment, using an  
10 alternative Lieber DeCarli diet containing different concentrations of pectin from apple (0.4%,  
11 1%, 2% and 6.5%, w/w, Sigma-Aldrich, Saint Quentin Fallavier, France). To treat mice by an  
12 AhR agonist, the 6-formylindolo (3,2-b)carbazole (Ficz; Sigma-Aldrich) was re-suspended in  
13 dimethyl sulfoxide (DMSO; Sigma-Aldrich), diluted in olive oil (Sigma-Aldrich) and  
14 administered intraperitoneally. Ficz (1 µg/mouse) treatment was injected three times during the  
15 last week when mice were exposed to the maximum dose of alcohol (5%) and until  
16 euthanization. Control mice received DMSO vehicle diluted in olive oil intraperitoneally alone  
17 for the Ficz treatment group.

18  
19 **Fecal microbiota transfer.** Mice received feces from alcoholic patients with severe alcoholic  
20 hepatitis as previously described [5, 24]. Two set of independent experiments were performed,  
21 a first set with feces from two different patients (F<sub>1</sub> and F<sub>2</sub>) and a second set with feces from  
22 one patient (F<sub>3</sub>). Briefly, feces from human patients were recovered and immediately stored at  
23 4°C in an anaerobiosis generator (Genbox, Biomérieux, Capronne, France) to favour the  
24 preservation of anaerobic bacteria. All samples were processed within 24 h. Feces were rapidly  
25 diluted 100-fold in Brain Heart Infusion (BHI, Becton Dickinson) supplemented with 0.5mg/ml  
26 L-cysteine (Sigma-Aldrich, St-Louis, MO, USA) and 20% skim milk (Becton Dickinson)  
27 (vol/vol) and stored in aliquots at -80°C. This ready-to-use fecal suspension was used for FMT  
28 to mice.

29 Mice were fasted 1 h and then subjected to bowel cleansing by oral-gastric gavage with PEG  
30 (polyethylene glycol, Macrogol 4000, Fortrans, Ipsen Pharma, France). Four hours later, mice  
31 received the human feces by oral gastric gavage (200 µl of resuspended feces prepared as  
32 described above). Mice were then allowed free access to food and water. FMT was repeated  
33 twice a week for four weeks. Bowel cleansing was only performed on day 1.

1 **Patients.** Two groups of patients were included in the study: patients with severe alcoholic  
2 hepatitis (sAH) and alcoholic patients without alcoholic hepatitis and without cirrhosis (noAH).  
3 All patients were admitted to the hepato-gastroenterology department of Antoine-Béclère  
4 University Hospital, Clamart, France. Alcoholic patients were eligible for inclusion if they had  
5 consumed at least 50 g of alcohol per day over the previous year, were negative for hepatitis B  
6 surface antigens, and seronegative for antibodies against hepatitis C virus (HCV). Exclusion  
7 criteria were gastrointestinal bleeding, bacterial infection, hepatocellular carcinoma or other  
8 carcinoma, acute pancreatitis, other severe associated disease, diabetes mellitus, dyslipidemia,  
9 presence of anti-HIV antibodies, and antibiotic or probiotic intake in the last 3 months. A  
10 standardized questionnaire was used, to collect information about alcohol consumption [25].  
11 Severe alcoholic hepatitis was suspected in patients with a Maddrey score  $> 32$  and was  
12 confirmed by a liver biopsy (histological score for AH  $\geq 6$  with neutrophilic infiltration)[26,  
13 27]. Feces from 3 independent patients with severe alcoholic hepatitis were used for the fecal  
14 transfer in mice.

15 The study was carried out in accordance with the Helsinki Declaration and was approved by the  
16 Ile de France VII ethics committee (Bicêtre Hospital, 94270 le Kremlin-Bicêtre, France). All  
17 the participants provided written informed consent.

18

19 **Statistical analyses.** Results are represented as the mean  $\pm$  SEM. Statistical comparison was  
20 performed by first testing the normality of the data using the Shapiro-Wilk test of normality and  
21 then performing unpaired Mann-Whitney, unpaired t-test, Kruskal-Wallis or ANOVA tests as  
22 appropriate (Graphpad Prism, Graphpad Software Inc, La Jolla, California, USA);  $p < 0,05$  was  
23 considered to be statistically significant. \* $p < 0.05$ , \*\* $p < 0.01$ , \*\*\* $p < 0.001$ .

24

25 *See the Supplementary section for the sources of materials and detailed methods.*

26

## 27 **RESULTS**

### 28 **Altering the intestinal microbiota reverses alcohol-induced liver lesions**

29 We tested whether altering the intestinal microbiota can reverse the progression of  
30 alcohol-induced liver lesions using human microbiota-associated mice (HMA) [24, 28]. We  
31 used HMA mice transplanted with the microbiota from sAH patients, as we have previously  
32 shown that the intestinal microbiota worsens alcohol-induced liver lesions in this model [5].  
33 Pectin, a dietary fiber known to favor the growth of specific bacterial genera, such as

1 *Bacteroides* [4, 29], which are reduced by alcohol intake [27], was used to alter the intestinal  
2 microbiota. Conventional (Alc) and HMA mice from three independent patients with sAH (Alc  
3 F<sub>1</sub>, Alc F<sub>2</sub>, Alc F<sub>3</sub>) were fed alcohol using the Lieber DeCarli (LDC) diet, as described  
4 previously [4] (**Fig. 1a**). The clinical characteristics of the donors with sAH are presented in  
5 **Supplementary Table 1**. Principal coordinate analysis (PCoA) showed that alcohol, human  
6 microbiota transfer, and pectin treatment induced changes in intestinal microbiota composition  
7 (unweighted Unifrac, ANOSIM,  $r = 0.59$ ,  $P < 0.001$ , **Fig. 1b and Supplementary Fig. 1a, c**).  
8 These changes included an increase in the *Bacteroides* genus in the pectin-treated group (**Fig.**  
9 **1c and Supplementary Fig. 1b, d**).

10 HMA alcohol-fed mice developed liver lesions during the first week of alcohol intake,  
11 as shown by liver TG accumulation and an increase in ALT levels and several markers of  
12 inflammation (**Supplementary Fig. 2 a-e**). At this point, mice were treated with pectin in order  
13 to alter intestinal microbiota. Pectin did not modify the alcohol absorption (**Fig 1a and**  
14 **Supplementary Fig. 2f**). Changing microbiota by using pectin, reversed alcohol-induced liver  
15 lesions in HMA mice fed alcohol. These mice (Alc F<sub>1</sub>P) had lower levels of ALT (**Fig. 1d**),  
16 liver TG (**Fig. 1e**), steatosis (**Fig. 1f**), and liver inflammation markers (*ccl2*, *tnfa*, *il1 $\beta$*  and *ccl3*)  
17 (**Fig. 1g**) than Alc F<sub>1</sub> and Alc mice. We obtained similar modifications of the intestinal  
18 microbiota and recovery of alcohol-induced liver lesions in HMA mice using feces from two  
19 other independent sAH patients (Alc F<sub>2</sub> and Alc F<sub>3</sub>, **Supplementary Fig. 3 and 4**).

20 Altering the intestinal microbiota using high-dose of fiber may be associated with poor  
21 tolerance (bloating, abdominal distension) [30]. We therefore tested the efficacy of lower doses  
22 of pectin on ALD. Two percent pectin induced similar changes of the alcohol-induced liver  
23 lesions and gut barrier function while improving treatment tolerance (**Supplementary Fig. 4**).  
24 Pectin treatment induced dose-dependent changes in the intestinal microbiota (**Supplementary**  
25 **Fig. 5a-d**). Among the specific changes observed in the LEfSe analysis, Alc F<sub>3</sub> P2 showed an  
26 increase in the abundance of the Bacteroidetes phylum, a decrease in the abundance of the  
27 Firmicutes phylum, and an increase in the abundance of *Bacteroides* and *Lactobacillus* genera,  
28 similar to that of Alc F<sub>3</sub> P6.5 relative to Alc F<sub>3</sub> (**Supplementary Fig. 5d**). However, the increase  
29 in the abundance of Proteobacteria and Enterobacteriaceae observed in the Alc F<sub>3</sub> P6.5 mice  
30 was not observed in the Alc F<sub>3</sub> P2 mice (**Supplementary Fig. 5e**).

31

32 **Altering the intestinal microbiota improves gut-barrier function in alcohol-fed human**  
33 **microbiota associated mice**

1 Disruption of the intestinal barrier correlates with the severity of liver injury in ALD [4,  
2 5, 6, 15, 31]. Alcohol-induced gut barrier disruption results in a decrease in the level of the  
3 antimicrobial peptides *reg3 $\beta$*  and *reg3 $\gamma$*  and mucus production [4, 6]. Restoration of these  
4 functions is required to improve alcohol-induced liver injury [4, 6, 16, 32]. Altering the  
5 intestinal microbiota improved liver injury through improvement of the gut barrier function, as  
6 shown by an increase in antimicrobial peptide (*reg3 $\beta$*  and *reg3 $\gamma$* ) mRNA levels in the colon and  
7 ileum, and the proportion of goblet cells (**Supplementary Fig. 6a-g**). This was associated with  
8 an improvement of intestinal permeability, as shown by an increase in tight junction proteins  
9 (*ZO-1* and *occludin*) as shown by mRNA levels and immunofluorescence in the colon and ileum  
10 (**Supplementary Fig. 6h-i and Supplementary Fig. 7**) and a decrease of bacterial  
11 translocation into the liver (**Supplementary Fig. 6j**). These results show that altering the  
12 microbiota improves the gut barrier and reverses alcohol-induced liver injury, despite on-going  
13 heavy alcohol consumption.

14

### 15 **Altering the intestinal microbiota modifies its functions and the fecal metabolome**

16 We next explored the functional impact of altering the intestinal microbiota using pectin  
17 by generating the predicted metagenome using Phylogenetic Investigation of Communities by  
18 Reconstruction of Unobserved States (PICRUSt) [33]. A total of 4,977 KEGG orthologs were  
19 assigned to 146 metabolic pathways and 115 structural complex modules. Pectin-treated mice  
20 showed a higher number of bacterial genes involved in carbohydrate, lipid, and amino-acid  
21 metabolism (**Fig. 2a**). Conversely, control mice showed a higher number of bacterial genes  
22 involved in amino-acid, energy, and cofactor and vitamin metabolism. We obtained similar  
23 predicted metagenome profiles in mice transplanted with the intestinal microbiota of the two  
24 other independent patients (F<sub>2</sub> and F<sub>3</sub>) (**Supplementary Table 2**).

25 We further studied whether such changes in the bacterial pathways induce alterations in  
26 the fecal metabolome by performing targeted metabolomic profiling. PCA and heatmaps  
27 showed that altering the intestinal microbiota induced a specific fecal metabolomic profile (**Fig.**  
28 **2b, c**). Enrichment analysis using Metabolom Analyst led to the identification of 52 pathways  
29 that were modified between Alc F<sub>1</sub> and Alc F<sub>1</sub> P mice (FDR < 0.05) (**Fig. 2d** and  
30 **Supplementary Table 3**). These pathways belong to the metabolism of amino acids (lysine,  
31 tyrosine, tryptophan, valine, leucine, isoleucine, and beta-alanine), carbohydrates (starch and  
32 sucrose, pentose and glucose interconversion, and ascorbate) lipids, and vitamins (biotin and  
33 ascorbate). Many of the changes in the fecal metabolomic pathways belong to those highlighted

1 by the predicted bacterial metagenome (**Fig. 2a, d**). These results were also confirmed when  
2 using lower doses of pectin (**Supplementary Fig. 8**).

3 Among the amino acids of which the levels were modified by pectin, we specifically  
4 identified a decrease in the levels of tryptophan and indole, precursors of microbiota-derived  
5 tryptophan metabolites (**Fig. 2e**). We then performed specific metabolomic profiling of  
6 tryptophan metabolites, as we observed an increase in the abundance of *Bacteroides*, taxa that  
7 can metabolize tryptophan into indole derivatives, in pectin-treated mice. We observed a  
8 decreased level of indole-3-acrylic acid in alcohol-fed conventional and HMA mice as  
9 compared to control mice and a decrease in overall AhR agonists (sum of 3-indoxyl sulfuric  
10 acid, 5-Methoxy-3-indoleacetic acid, indole-3-acetic acid, indole-3-acrylic acid, indole-3-  
11 aldehyde, indole-3-lactic acid, indole-3-propionic acid) in alcohol-fed HMA mice. These  
12 changes were restored after pectin treatment with an overall increase in total AhR agonists in  
13 pectin treated mice (**Fig. 2f**).

14

### 15 **Activation of the AhR pathway improves alcohol-induced liver injury**

16 Altering the intestinal microbiota with pectin in the HMA mouse model of ALD reverses  
17 alcohol-induced injury and is associated with changes in the microbiota and tryptophan  
18 metabolism. We therefore studied the role of the AhR pathway, which can be activated by  
19 bacterial tryptophan metabolites. We analyzed the expression of *cyp1a1* and its repressor *ahrr*,  
20 target genes of AhR activation in the colon. Their expression in the colon (**Fig. 3a**), together  
21 with that of *il22* [20] and *il17* (**Fig. 3b**), which are also controlled by AhR activation [34],  
22 increased after altering the intestinal microbiota by pectin treatment. We then assessed the direct  
23 involvement of AhR in the improvement of alcohol-induced injury by treating mice with an  
24 AhR agonist, 6-formylindolo (3,2-b) carbazole (Ficz). Treatment of Alc mice with Ficz  
25 increased the expression of AhR target genes *Cyp1a1* and *Scd1* in the liver (**Fig. 3c**) and  
26 decreased alcohol-induced liver lesions, with a decrease in ALT, liver TG, and inflammatory  
27 marker levels (**Fig. 3d, e**). Treatment with Ficz also increased antimicrobial peptide levels in  
28 the colon and ileum (**Fig. 3f, g**) but only the expression of *Reg3γ* in the ileum reached statistical  
29 significance, simulating the effects of pectin. We next tested whether AhR signaling mediates  
30 the effects of pectin using alcohol-fed mice deficient for AhR (AhR KO). Although pectin  
31 treatment still restored ALT levels in alcohol-fed AhR KO mice, it could neither alleviate  
32 steatosis (**Fig. 4a, b**) nor restore *cyp1a1* and *ahrr* mRNA levels (**Fig. 4c**). Accordingly,  
33 restoration of *il22*, *reg3β*, and *reg3γ* mRNA levels by pectin treatment was also abrogated (**Fig.**

1 **4d)**. Overall, these data show that the effects of pectin are, at least partially, mediated by AhR  
2 pathways.

3

#### 4 **Tryptophan metabolism is impaired in patients with severe alcoholic hepatitis**

5 We next explored the relevance of impaired tryptophan metabolism in the context of  
6 human disease and analyzed fecal and serum samples of alcoholic patients with (sAH) or  
7 without alcoholic hepatitis (noAH) (**Supplementary Table 4**). There were no differences in the  
8 fecal levels of tryptophan, kynurenine, or AhR agonists between alcoholic patients, regardless  
9 of the severity of the liver injury (noAH or sAH) (data not shown). There was also no difference  
10 in the serum level of kynurenine between alcoholic patients (**Fig. 5a**). Conversely, serum levels  
11 of tryptophan and AhR agonists were lower in sAH patients than in noAH patients (**Fig. 5a**).  
12 We also found negative correlations between serum levels of Trp and AST ( $r = -0.6$ ,  $p < 0.01$ ),  
13 bilirubin ( $r = -0.7$ ,  $p < 0.001$ ), prothrombin time ( $r = -0.7$ ,  $p < 0.001$ ), and MELD score ( $r = -$   
14  $0.6$ ,  $p < 0.001$ ) (**Fig. 5b**). This suggest that tryptophan metabolism is impaired in patients with  
15 alcoholic hepatitis and that the modulation of AhR could be a new therapeutic target.

## 1 DISCUSSION

2 The IM plays a role in the pathophysiology of ALD and bacterial composition  
3 contributes to the severity of liver injury, independently of alcohol intake [2, 5]. Bacteria  
4 interact directly with the host and indirectly through a large panel of bacterial metabolites [35].  
5 Impairment of several bacterial metabolic functions has been shown to exacerbate ALD,  
6 including that of bacterial synthesis of saturated long-chain fatty acids [36], bile acids [5, 19,  
7 27], and tryptophan [37]. In ALD, disruption of the intestinal barrier correlates with the severity  
8 of liver lesions [4, 15, 31]. The role of the IM in the development of a leaky gut is associated  
9 with decreased levels of antimicrobial Reg 3 peptides and decreased mucus production [4, 16].  
10 Altering the IM using probiotics or prebiotics in murine models can prevent ALD by modulating  
11 these functions [6, 10, 38, 39, 40]. Specifically, pectin, a fiber that modulates the intestinal  
12 microbiota, can prevent alcohol-induced liver injury by improving gut barrier function [4].  
13 Nevertheless, a preventive effect of such a treatment is not relevant for patients with alcohol-  
14 use disorders that have ALD. Therefore, we addressed the effect of pectin in a mouse model of  
15 ongoing alcohol administration after the onset of liver injury. We focused on bacterial indole  
16 derivatives, as the molecular mechanisms by which fiber-induced changes of the IM improve  
17 ALD have not been elucidated.

18 Here, we show that pectin, used as a curative treatment, is able to reverse alcohol-  
19 induced liver injury in the context of the human microbiota. We used HMA transplanted with  
20 the feces of alcoholic patients with sAH. Liver injury in these mice is worse than that of  
21 wildtype alcohol-fed mice. Improvement of liver lesions is associated with improved gut barrier  
22 function, including the restoration of mucus production and antimicrobial Reg 3 peptide levels.  
23 Pectin, as a dietary fiber, is known to favor the growth of specific bacterial genera, such as  
24 *Bacteroides* [4, 29]. In alcoholic patients, sAH is associated with a decrease in the abundance  
25 of Bacteroidetes and changes in IM function [5, 41]. A similar decrease in the abundance of  
26 Bacteroidetes has also been observed in animal models of ALD [4]. Here, we show that pectin  
27 induces an increase in the abundance of *Bacteroides*, regardless of the effective dose.

28 A high dose of pectin (6.5%) was also associated with an increased abundance of  
29 Proteobacteria, which could pose safety concerns, as several species of this phylum are  
30 considered to be opportunistic pathogens [42]. Moreover, fermentable fiber (including pectin)  
31 has been reported to induce an increase in the abundance of Proteobacteria and hepatocarcinoma  
32 in several animal models (TLR5, TLR4, and Lcn2 –deficient mice). This is due to the inability  
33 of the innate immunity in the gut to prevent the translocation of Proteobacteria species [43].  
34 However, in our study, the lower dose of pectin (2%) used to improve intestinal tolerance to a

1 diet rich in fiber abrogated Proteobacteria overgrowth and achieved the beneficial effects that  
2 we observed on alcohol-induced liver lesions with a pectin-enriched diet. The amount of pectin  
3 to administrate in patients to match the minimal effective dose described in our study (2%)  
4 would be of 40 g/day. Of note, the recommended daily dose of fiber intake ranges between 30-  
5 38 g/day in men and 21-25 g/day in women [44]. Nevertheless, the amount of fiber consumed  
6 by humans is dependent on their diet. It has been suggested that omnivores consumed less than  
7 23 g of fibers/day, vegetarians significantly more (37 g/day) and vegans the most (47 g/day)  
8 [45]. Patients with chronic liver disease (viral and alcoholic cirrhosis) have a lower intake of  
9 vegetables which are rich in fibers [46]. Moreover, a high-fiber diet has been related to  
10 regression of NAFLD [47] and recent epidemiological data showed that dietary fiber intake,  
11 especially soluble fibers (such as pectin), is inversely associated with the risk of several chronic  
12 diseases and with mortality [48]. Studies investigating pectin administration in different  
13 conditions used up to 60 g/day and reported good tolerance [49]. The main side effect was  
14 bloating but individual sensitivity to develop side effects is highly variable [50]. These data  
15 suggest that a moderate amount of pectin may be a promising and safe alimentary complement  
16 in the management of alcoholic patients.

17 We further analyzed intestinal metabolites to investigate the mechanisms by which  
18 pectin-induced modifications of the IM reduce alcohol-induced gut and liver injuries. The  
19 microbiota reshaped by pectin harbored more genes involved in amino-acid and xenobiotic  
20 metabolism. This metagenomic prediction was confirmed by the quantification of fecal  
21 metabolites. We specifically identified a decrease in tryptophan levels and an increase in the  
22 level of indole derivatives. These metabolites are only produced by the intestinal microbiota  
23 from tryptophan [37]. Several microbiota-derived tryptophan metabolites are able to activate  
24 the AhR, thus playing a key role in gut homeostasis through the regulation of anti-microbial  
25 peptide and mucus production by IL-22 [21]. Moreover, it has been previously shown that IL-  
26 22 is down-regulated in alcohol-fed mice and oral treatment with recombinant IL-22 or bacteria  
27 that produce this cytokine prevents alcohol-induced liver injury [37, 51]. AhR activation has  
28 been shown to improve inflammatory bowel disease [52] and metabolic syndrome [37, 53, 54].  
29 Moreover, hepatic AhR activation prevents HSC activation and the expression of genes required  
30 for liver fibrogenesis by disrupting the interaction of Smad3 with  $\beta$ -catenin [55]. Here, we show  
31 that the improvement of mucus and antimicrobial peptide production by pectin is associated  
32 with the restoration of AhR-responsive gene expression, including that of IL-22, *Cyp1a1*, and  
33 *ahrr*. Conversely, low levels of *reg3 $\beta$* , *reg3 $\gamma$* , and mucus production in untreated alcohol-fed  
34 mice correlated with lower levels of *il22*, *Cyp1a1*, and *ahrr*.



1 We also treated mice with an AhR agonist, FICZ, to address the direct involvement of  
2 AhR in the effects of pectin. FICZ treatment was sufficient to mediate a reduction in alcohol-  
3 induced injury. In contrast, pectin treatment of AhR-deficient alcohol-fed mice had only a  
4 minimal effect on alcohol-induced liver lesions suggesting that the effects of pectin treatment  
5 in our model of ALD are not solely mediated by AhR. Indeed, pectin induces broad changes  
6 at the microbial and metabolomic level and other mechanisms independent of AhR could also  
7 mediate the effect observed in our study.

8 The relevance of impaired tryptophan metabolism in the context of human disease was  
9 confirmed by reduced serum levels of tryptophan and AhR agonists in patients with sAH.  
10 Conversely, there were no differences in the fecal levels of tryptophan, kynurenine, or AhR  
11 agonists between alcoholic patients, regardless of the severity of the liver injury (noAH or sAH).  
12 However, it has been reported that patients with alcoholic hepatitis have lower levels of fecal  
13 indole-3-acetic acid and indole-3-lactic acid than healthy patients who do not consume alcohol  
14 [37]. These discrepancies suggest that alcohol induces impairment of tryptophan metabolism  
15 independently of liver disease.

16 Our results provide the basis for further studies in patients with ALD that will aim to  
17 correct the AhR-ligand deficiency. Indeed, it has been recently shown that *Lactobacillus*  
18 *reuteri*, which is known to produce AhR agonists, improves ALD [37], as well as treatment  
19 with a direct agonist, such as indole-3 acetic acid. Moreover, treatment with *Lactobacillus*  
20 *reuteri* can also improve metabolic syndrome [53] and colitis [56, 57] in animal models. Indole-  
21 3-pyruvic acid, an AhR agonist, improves experimental colitis [58] and indigo, a tryptophan  
22 metabolite that activates the AhR, is effective in inducing remission in patients with ulcerative  
23 colitis [59].

24 In conclusion, our study shows that alcohol-induced liver lesions can be reversed by  
25 modifying AhR-agonist production by the IM. As there is no treatment that can reverse alcohol-  
26 induced liver lesions other than liver transplant, modulation of the AhR pathways by  
27 supplementation with prebiotics, AhR ligand-producing bacteria, or pharmacological AhR  
28 ligands, may hold promise in the development of new therapeutic approaches to ALD.

1 **Acknowledgments.** The authors thank Mylène Levant, Baptiste Lecomte, and Sarah Mendez  
2 for follow-up of the mice, the Plaimmo Platform, PHIC platform (Morgan Ocimek and Séverine  
3 Domenichini), and Nicolas Sorhaindo for plasma quantification (Plateforme de Biochimie,  
4 Bichat). We also thank the NED team (Olivier Zemb and Béatrice Gabinaud) and the GeT-  
5 PlaGe platform for their help with the sequencing data.

6  
7 **Disclosures:** DC received travel funds from Biocodex and Gilead, lecture fees from Gilead, and  
8 royalties from John Libbey Eurotext. HS received unrestricted study grants from Danone,  
9 Biocodex, and Enterome and board membership, consultancy, or lecture fees from Carenity,  
10 Abbvie, Astellas, Danone, Ferring, Mayoly Spindler, MSD, Novartis, Roche, Tillots, Enterome,  
11 Maat, BiomX, Biose, Novartis, and Takeda and is a co-founder of Exeliom Biosciences. GP  
12 received travel funds from Janssen and Gilead, consulting fees from Bayer, Biocodex, Roche,  
13 Gilead, Pierre Fabre, and Servier, and royalties from Elsevier-Masson, Solar,  
14 Flammation/Versilio, and John Libbey Eurotext. AMC received travel funds and consulting  
15 fees from Biocodex and royalties from Elsevier-Masson, Solar, Flammation/Versilio, and John  
16 Libbey Eurotext. All other authors declare no conflicts of interest.

17

18 **Financial support:** This work was supported by INSERM, Université Paris-Sud, "Fondation  
19 pour la recherche médicale" (FRM), the National French Society of Gastroenterology  
20 (SNFGE), "Association Française pour l'Etude du Foie" (AFEF), "Fondation pour la Recherche  
21 en Alcoologie" (FRA/IREB), "Institut de Recherches Internationales Servier" (IRIS), and  
22 "Groupement transversal INSERM sur le microbiote" (GPT microbiota). DC received a grant  
23 from Biocodex. MSp received a grant from the Laboratory of Excellence LERMIT supported  
24 by the "Agence Nationale de la Recherche" (ANR-10-LABX-33). MD received a grant from  
25 FRM. CHo received a CIFRE (Conventions Industrielles de Formation par la Recherche)  
26 scholarship in collaboration with the IRIS. HS received funding from the European Research  
27 Council (ERC) under the European Union's Horizon 2020 Research and Innovation Programme  
28 (ERC-2016-StG-71577).

29

30 **Authors' Contributions:** LW and DC: contributed equally to this work for the study concept  
31 and design, acquisition, analysis, and interpretation of data, and drafting of the manuscript.  
32 CHu, MSp, CHo, VLLM, VP, GF, NT and MSt: technical support. MD and FMN: histological  
33 analysis. SD and GK: fecal metabolite quantification. CSV: provided patients. HS: provided

- 1 AhR KO mice. HS and PE: tryptophan metabolite analysis. GP: critical revision of the
- 2 manuscript, obtained funding, and provided patients. AMC: study concept, design, and
- 3 supervision, analysis and interpretation of the data, drafting of the manuscript, and funding
- 4 raising.

**1 REFERENCES**

- 2 1 Collaborators GBDA. Alcohol use and burden for 195 countries and territories, 1990-  
3 2016: a systematic analysis for the Global Burden of Disease Study 2016. *Lancet*  
4 2018;**392**:1015-35.
- 5 2 Seitz HK, Bataller R, Cortez-Pinto H, Gao B, Gual A, Lackner C, *et al.* Alcoholic liver  
6 disease. *Nat Rev Dis Primers* 2018;**4**:16.
- 7 3 Chen Y, Yang F, Lu H, Wang B, Lei D, Wang Y, *et al.* Characterization of fecal  
8 microbial communities in patients with liver cirrhosis. *Hepatology* 2011;**54**:562-72.
- 9 4 Ferrere G, Wrzosek L, Cailleux F, Turpin W, Puchois V, Spatz M, *et al.* Fecal  
10 microbiota manipulation prevents dysbiosis and alcohol-induced liver injury in mice. *J Hepatol*  
11 2017;**66**:806-15.
- 12 5 Llopis M, Cassard AM, Wrzosek L, Bosch L, Bruneau A, Ferrere G, *et al.* Intestinal  
13 microbiota contributes to individual susceptibility to alcoholic liver disease. *Gut* 2016;**65**:830-  
14 9.
- 15 6 Yan AW, Fouts DE, Brandl J, Starkel P, Torralba M, Schott E, *et al.* Enteric dysbiosis  
16 associated with a mouse model of alcoholic liver disease. *Hepatology* 2011;**53**:96-105.
- 17 7 Duan Y, Llorente C, Lang S, Brandl K, Chu H, Jiang L, *et al.* Bacteriophage targeting  
18 of gut bacterium attenuates alcoholic liver disease. *Nature* 2019;**575**:505-11.
- 19 8 Llorente C, Jepsen P, Inamine T, Wang L, Bluemel S, Wang HJ, *et al.* Gastric acid  
20 suppression promotes alcoholic liver disease by inducing overgrowth of intestinal  
21 *Enterococcus*. *Nat Commun* 2017;**8**:837.
- 22 9 Philips CA, Pande A, Shasthry SM, Jamwal KD, Khillan V, Chandel SS, *et al.* Healthy  
23 Donor Fecal Microbiota Transplantation in Steroid-Ineligible Severe Alcoholic Hepatitis: A  
24 Pilot Study. *Clin Gastroenterol Hepatol* 2017;**15**:600-2.
- 25 10 Grander C, Adolph TE, Wieser V, Lowe P, Wrzosek L, Gyongyosi B, *et al.* Recovery  
26 of ethanol-induced *Akkermansia muciniphila* depletion ameliorates alcoholic liver disease. *Gut*  
27 2017.
- 28 11 Seo B, Jeon K, Moon S, Lee K, Kim WK, Jeong H, *et al.* *Roseburia* spp. Abundance  
29 Associates with Alcohol Consumption in Humans and Its Administration Ameliorates  
30 Alcoholic Fatty Liver in Mice. *Cell Host Microbe* 2020;**27**:25-40 e6.
- 31 12 Bajaj JS. Alcohol, liver disease and the gut microbiota. *Nat Rev Gastroenterol Hepatol*  
32 2019;**16**:235-46.
- 33 13 Cassard AM, Ciocan D. Microbiota, a key player in alcoholic liver disease. *Clin Mol*  
34 *Hepatol* 2018;**24**:100-7.
- 35 14 Rao R. Endotoxemia and gut barrier dysfunction in alcoholic liver disease. *Hepatology*  
36 2009;**50**:638-44.
- 37 15 Chen P, Starkel P, Turner JR, Ho SB, Schnabl B. Dysbiosis-induced intestinal  
38 inflammation activates TNFRI and mediates alcoholic liver disease in mice. *Hepatology*  
39 2015;**61**:883-94.
- 40 16 Hartmann P, Chen P, Wang HJ, Wang L, McCole DF, Brandl K, *et al.* Deficiency of  
41 intestinal mucin-2 ameliorates experimental alcoholic liver disease in mice. *Hepatology*  
42 2013;**58**:108-19.
- 43 17 Yoseph BP, Breed E, Overgaard CE, Ward CJ, Liang Z, Wagener ME, *et al.* Chronic  
44 alcohol ingestion increases mortality and organ injury in a murine model of septic peritonitis.  
45 *PLoS One* 2013;**8**:e62792.
- 46 18 Bajaj JS, Hylemon PB. Gut-liver axis alterations in alcoholic liver disease: Are bile acids  
47 the answer? *Hepatology* 2018;**67**:2074-5.
- 48 19 Hartmann P, Hochrath K, Horvath A, Chen P, Seebauer CT, Llorente C, *et al.*  
49 Modulation of the intestinal bile acid/farnesoid X receptor/fibroblast growth factor 15 axis  
50 improves alcoholic liver disease in mice. *Hepatology* 2018;**67**:2150-66.

- 1 20 Lee JS, Cella M, McDonald KG, Garlanda C, Kennedy GD, Nukaya M, *et al.* AHR  
2 drives the development of gut ILC22 cells and postnatal lymphoid tissues via pathways  
3 dependent on and independent of Notch. *Nat Immunol* 2011;**13**:144-51.
- 4 21 Zelante T, Iannitti RG, Cunha C, De Luca A, Giovannini G, Pieraccini G, *et al.*  
5 Tryptophan catabolites from microbiota engage aryl hydrocarbon receptor and balance mucosal  
6 reactivity via interleukin-22. *Immunity* 2013;**39**:372-85.
- 7 22 Zheng Y, Valdez PA, Danilenko DM, Hu Y, Sa SM, Gong Q, *et al.* Interleukin-22  
8 mediates early host defense against attaching and effacing bacterial pathogens. *Nat Med*  
9 2008;**14**:282-9.
- 10 23 Badawy AA, Morgan CJ, Lovett JW, Bradley DM, Thomas R. Decrease in circulating  
11 tryptophan availability to the brain after acute ethanol consumption by normal volunteers:  
12 implications for alcohol-induced aggressive behaviour and depression. *Pharmacopsychiatry*  
13 1995;**28 Suppl 2**:93-7.
- 14 24 Wrzosek L, Ciocan D, Borentain P, Spatz M, Puchois V, Hugot C, *et al.* Transplantation  
15 of human microbiota into conventional mice durably reshapes the gut microbiota. *Sci Rep*  
16 2018;**8**:6854.
- 17 25 Williams GD, Proudfit AH, Quinn EA, Campbell KE. Variations in quantity-frequency  
18 measures of alcohol consumption from a general population survey. *Addiction* 1994;**89**:413-  
19 20.
- 20 26 Alcoholic liver disease: morphological manifestations. Review by an international  
21 group. *Lancet* 1981;**1**:707-11.
- 22 27 Ciocan D, Voican CS, Wrzosek L, Hugot C, Rainteau D, Humbert L, *et al.* Bile acid  
23 homeostasis and intestinal dysbiosis in alcoholic hepatitis. *Aliment Pharmacol Ther* 2018.
- 24 28 Le Roy T, Debedat J, Marquet F, Da-Cunha C, Ichou F, Guerre-Millo M, *et al.*  
25 Comparative Evaluation of Microbiota Engraftment Following Fecal Microbiota Transfer in  
26 Mice Models: Age, Kinetic and Microbial Status Matter. *Front Microbiol* 2018;**9**:3289.
- 27 29 Dongowski G, Lorenz A, Proll J. The degree of methylation influences the degradation  
28 of pectin in the intestinal tract of rats and in vitro. *The Journal of nutrition* 2002;**132**:1935-44.
- 29 30 Cummings JH, Macfarlane GT, Englyst HN. Prebiotic digestion and fermentation. *Am*  
30 *J Clin Nutr* 2001;**73**:415S-20S.
- 31 31 Mathurin P, Deng QG, Keshavarzian A, Choudhary S, Holmes EW, Tsukamoto H.  
32 Exacerbation of alcoholic liver injury by enteral endotoxin in rats. *Hepatology* 2000;**32**:1008-  
33 17.
- 34 32 Wang L, Fouts DE, Starkel P, Hartmann P, Chen P, Llorente C, *et al.* Intestinal REG3  
35 Lectins Protect against Alcoholic Steatohepatitis by Reducing Mucosa-Associated Microbiota  
36 and Preventing Bacterial Translocation. *Cell Host Microbe* 2016;**19**:227-39.
- 37 33 Langille MG, Zaneveld J, Caporaso JG, McDonald D, Knights D, Reyes JA, *et al.*  
38 Predictive functional profiling of microbial communities using 16S rRNA marker gene  
39 sequences. *Nat Biotechnol* 2013;**31**:814-21.
- 40 34 Hayes MD, Ovcinnikovs V, Smith AG, Kimber I, Dearman RJ. The aryl hydrocarbon  
41 receptor: differential contribution to T helper 17 and T cytotoxic 17 cell development. *PLoS*  
42 *One* 2014;**9**:e106955.
- 43 35 Postler TS, Ghosh S. Understanding the Holobiont: How Microbial Metabolites Affect  
44 Human Health and Shape the Immune System. *Cell Metab* 2017;**26**:110-30.
- 45 36 Chen P, Torralba M, Tan J, Embree M, Zengler K, Starkel P, *et al.* Supplementation of  
46 Saturated Long-Chain Fatty Acids Maintains Intestinal Eubiosis and Reduces Ethanol-induced  
47 Liver Injury in Mice. *Gastroenterology* 2015;**148**:203-14 e16.
- 48 37 Hendrikx T, Duan Y, Wang Y, Oh JH, Alexander LM, Huang W, *et al.* Bacteria  
49 engineered to produce IL-22 in intestine induce expression of REG3G to reduce ethanol-  
50 induced liver disease in mice. *Gut* 2018.

- 1 38 Bull-Otterson L, Feng W, Kirpich I, Wang Y, Qin X, Liu Y, *et al.* Metagenomic analyses  
2 of alcohol induced pathogenic alterations in the intestinal microbiome and the effect of  
3 *Lactobacillus rhamnosus* GG treatment. PLoS One 2013;**8**:e53028.
- 4 39 Chen RC, Xu LM, Du SJ, Huang SS, Wu H, Dong JJ, *et al.* *Lactobacillus rhamnosus*  
5 GG supernatant promotes intestinal barrier function, balances Treg and TH17 cells and  
6 ameliorates hepatic injury in a mouse model of chronic-binge alcohol feeding. Toxicol Lett  
7 2016;**241**:103-10.
- 8 40 Wang Y, Liu Y, Kirpich I, Ma Z, Wang C, Zhang M, *et al.* *Lactobacillus rhamnosus* GG  
9 reduces hepatic TNFalpha production and inflammation in chronic alcohol-induced liver injury.  
10 J Nutr Biochem 2013;**24**:1609-15.
- 11 41 Ciocan D, Rebours V, Voican CS, Wrzosek L, Puchois V, Cassard AM, *et al.*  
12 Characterization of intestinal microbiota in alcoholic patients with and without alcoholic  
13 hepatitis or chronic alcoholic pancreatitis. Sci Rep 2018;**8**:4822.
- 14 42 Shin NR, Whon TW, Bae JW. Proteobacteria: microbial signature of dysbiosis in gut  
15 microbiota. Trends Biotechnol 2015;**33**:496-503.
- 16 43 Singh V, Yeoh BS, Chassaing B, Xiao X, Saha P, Aguilera Olvera R, *et al.* Dysregulated  
17 Microbial Fermentation of Soluble Fiber Induces Cholestatic Liver Cancer. Cell 2018;**175**:679-  
18 94 e22.
- 19 44 Medicine Institute. Dietary Reference Intakes for Energy, Carbohydrate, Fiber, Fat,  
20 Fatty Acids, Cholesterol, Protein, and Amino Acids. 2005.
- 21 45 Davies GJ, Crowder M, Dickerson JW. Dietary fibre intakes of individuals with  
22 different eating patterns. Hum Nutr Appl Nutr 1985;**39**:139-48.
- 23 46 Buscail C, Bourcier V, Fezeu LK, Roulot D, Brule S, Ben-Abdesselam Z, *et al.* Eating  
24 Patterns in Patients with Compensated Cirrhosis: A Case-Control Study. Nutrients 2018;**10**.
- 25 47 Alferink LJM, Erler NS, de Kneegt RJ, Janssen HLA, Metselaar HJ, Darwish Murad S,  
26 *et al.* Adherence to a plant-based, high-fibre dietary pattern is related to regression of non-  
27 alcoholic fatty liver disease in an elderly population. Eur J Epidemiol 2020.
- 28 48 Partula V, Deschasaux M, Druesne-Pecollo N, Latino-Martel P, Desmetz E, Chazelas  
29 E, *et al.* Associations between consumption of dietary fibers and the risk of cardiovascular  
30 diseases, cancers, type 2 diabetes, and mortality in the prospective NutriNet-Sante cohort. Am  
31 J Clin Nutr 2020;**112**:195-207.
- 32 49 Seyrig JA, Naveau S, Gonzales R, Petit R. Pectines. Gastroenterol Clin Biol  
33 1983;**7**:1031-37.
- 34 50 Ralphs DNL, Lawaetz NJG. Effect of dietary fibre on gastric emptying in dumpers. Gut  
35 1978;**19**:986-87.
- 36 51 Ki SH, Park O, Zheng M, Morales-Ibanez O, Kolls JK, Bataller R, *et al.* Interleukin-22  
37 treatment ameliorates alcoholic liver injury in a murine model of chronic-binge ethanol feeding:  
38 role of signal transducer and activator of transcription 3. Hepatology 2010;**52**:1291-300.
- 39 52 Lamas B, Richard ML, Leducq V, Pham HP, Michel ML, Da Costa G, *et al.* CARD9  
40 impacts colitis by altering gut microbiota metabolism of tryptophan into aryl hydrocarbon  
41 receptor ligands. Nat Med 2016;**22**:598-605.
- 42 53 Natividad JM, Agus A, Planchais J, Lamas B, Jarry AC, Martin R, *et al.* Impaired Aryl  
43 Hydrocarbon Receptor Ligand Production by the Gut Microbiota Is a Key Factor in Metabolic  
44 Syndrome. Cell Metab 2018.
- 45 54 Wang X, Ota N, Manzanillo P, Kates L, Zavala-Solorio J, Eidenschenk C, *et al.*  
46 Interleukin-22 alleviates metabolic disorders and restores mucosal immunity in diabetes. Nature  
47 2014;**514**:237-41.
- 48 55 Yan J, Tung HC, Li S, Niu Y, Garbacz WG, Lu P, *et al.* Aryl Hydrocarbon Receptor  
49 Signaling Prevents Activation of Hepatic Stellate Cells and Liver Fibrogenesis in Mice.  
50 Gastroenterology 2019.

- 1 56 Mackos AR, Galley JD, Eubank TD, Easterling RS, Parry NM, Fox JG, *et al.* Social  
2 stress-enhanced severity of *Citrobacter rodentium*-induced colitis is CCL2-dependent and  
3 attenuated by probiotic *Lactobacillus reuteri*. *Mucosal Immunol* 2016;**9**:515-26.
- 4 57 Ahl D, Liu H, Schreiber O, Roos S, Phillipson M, Holm L. *Lactobacillus reuteri*  
5 increases mucus thickness and ameliorates dextran sulphate sodium-induced colitis in mice.  
6 *Acta Physiol (Oxf)* 2016;**217**:300-10.
- 7 58 Aoki R, Aoki-Yoshida A, Suzuki C, Takayama Y. Indole-3-Pyruvic Acid, an Aryl  
8 Hydrocarbon Receptor Activator, Suppresses Experimental Colitis in Mice. *J Immunol*  
9 2018;**201**:3683-93.
- 10 59 Naganuma M. Treatment with indigo naturalis for inflammatory bowel disease and other  
11 immune diseases. *Immunol Med* 2019:1-6.  
12

1 **FIGURE LEGENDS**

2

3 **Figure 1. Altering the intestinal microbiota using pectin reverses alcohol induced liver**  
4 **lesions.** Alc, alcohol-fed mice; Ctrl, control-fed mice; Alc F<sub>1</sub>, alcohol-fed mice humanized with  
5 the microbiota from a patient with severe alcoholic hepatitis (sAH, patient F<sub>1</sub>); Alc F<sub>1</sub> P,  
6 alcohol-fed mice humanized with microbiota from a patient with sAH (patient F<sub>1</sub>) and treated  
7 with 6.5% pectin. (a) Experimental design: mice were progressively adapted to a semi-liquid,  
8 Lieber DeCarli (LDC) diet, then an ethanol diet (1-3%), and finally fed a 5% ethanol diet for  
9 one week. Pectin was introduced in the diet at the same time as the 5% ethanol. Microbiota  
10 analysis: (b) PCoA plot, showing the unweighted UniFrac distance ( $p < 0.001$ ,  $R = 0.58$ ,  
11 ANOSIM test, 10,000 permutations, using the first 5 PC); (c) LDA effect size (LEfSe)  
12 cladograms showing the taxa most differentially associated with Alc F<sub>1</sub> (red) or Alc F<sub>1</sub> P mice  
13 (yellow) (Wilcoxon rank-sum test). Circle sizes in the cladogram plot are proportional to  
14 bacterial abundance. The circles represent, going from the inner to outer circle: phyla, genus,  
15 class, order, and family. (d) ALT level in Ctrl (n = 8), Alc (n = 8), Alc F<sub>1</sub> (n = 12), and Alc F<sub>1</sub>P  
16 (n = 10) mice. (e) Liver triglyceride quantification in Ctrl (n = 8), Alc (n = 8), Alc F<sub>1</sub> (n = 12),  
17 and Alc F<sub>1</sub>P (n = 10) mice. (f) Representative images of liver sections stained with hematoxylin-  
18 eosin, scale bar 100  $\mu$ m. (g) Liver mRNA levels determined by qPCR: *ccl2*, *tnfa*, *il1 $\beta$* , and *ccl3*  
19 normalized to that of the *gapdh* gene in Ctrl (n = 4), Alc (n = 5), Alc F<sub>1</sub> (n = 12), and Alc F<sub>1</sub>P  
20 (n = 10) mice. Results (d-g) are shown as the mean  $\pm$  SEM. Significant results for \* $p < 0.05$ ,  
21 \*\* $p < 0.01$ , and \*\*\* $p < 0.001$  were determined by Mann-Whitney tests unless stated otherwise.

22

23 **Figure 2. Functions of the intestinal microbiota and fecal metabolome are modified by**  
24 **pectin treatment.** Ctrl, control-fed mice; Alc, alcohol-fed mice; Alc F<sub>1</sub> and Alc F<sub>3</sub>, alcohol-fed  
25 mice humanized with microbiota from a patient with sAH (patients F<sub>1</sub> or F<sub>3</sub>); Alc F<sub>1</sub>P and Alc  
26 F<sub>3</sub>P, alcohol-fed mice humanized with microbiota from a patient with sAH (patients F<sub>1</sub> or F<sub>3</sub>)  
27 and treated with 6.5% pectin (F<sub>1</sub>) or 2% pectin (F<sub>3</sub>). (a) LEfSe cladograms of KEGG pathway  
28 contributions of predicted metagenomic data in Alc F<sub>1</sub> and Alc F<sub>1</sub>P mice (Wilcoxon rank-sum  
29 test). In a: Ctrl n = 8, Alc n = 10, Alc F<sub>1</sub> n = 14, and Alc F<sub>1</sub>P n = 10 mice per experiment. (b)  
30 PCA ordination plot on all fecal metabolomic data (147 metabolites). (c) Heatmap showing the  
31 first 60 metabolites ranked by t-tests between Alc F<sub>1</sub> (red) and Alc F<sub>1</sub>P (green). (d) Metabolic  
32 enrichment analysis showing the most altered pathways in Alc F<sub>1</sub>P mice relative to Alc F<sub>1</sub> mice.  
33 All matched pathways are displayed as circles. The color and size of each circle are based on  
34 the p value and pathway impact value, respectively. The graph was obtained by plotting the



1  $-\log$  of  $p$  values from the pathway enrichment analysis on the y axis and the pathway impact  
 2 values, derived from the pathway topology analysis, on the x axis. (e) Relative fecal levels of  
 3 tryptophan, kynurenine, and indole. In **b-e**: Ctrl  $n = 8$ , Alc  $n = 10$ , Alc F<sub>1</sub>  $n = 11$ , and Alc F<sub>1</sub>P  $n$   
 4  $= 7$  mice per group. (f) Tryptophan metabolites quantification in faeces. Aryl hydrocarbon  
 5 receptor (AhR) ligands (methyl-indole 3-acetic acid, indole 3-propionic acid, indole 3-  
 6 aldehyde, indole 3-acrylic acid, and 3-indoxyl sulfuric acid). In **f**: Ctrl  $n = 8$ , Alc  $n = 9$ , Alc F<sub>3</sub>  
 7  $n = 6$ , and Alc F<sub>3</sub>P  $n = 8$  mice per group. \* $p < 0.05$ , \*\* $p < 0.01$ , \*\*\* $p < 0.001$  by the ANOVA or  
 8 Kruskal-Wallis test with Tukey or Dunn correction for multiple comparisons, as appropriated.

9

10 **Figure 3. AhR activation reverses alcohol-induced liver lesions.** Ctrl, control-fed mice; Alc,  
 11 alcohol-fed mice. (a,b) Alc F<sub>3</sub>, alcohol-fed mice humanized with the microbiota from a patient  
 12 with sAH (patient F<sub>3</sub>); Alc F<sub>3</sub> P2, Alc F<sub>3</sub> P6.5, alcohol-fed mice humanized with the microbiota  
 13 from a patient with sAH (patient F<sub>3</sub>) and treated with 2 or 6.5% pectin. Colon mRNA levels  
 14 were determined by qPCR: (a) *cyp1a1* and *ahrr*, (b) *il17* and *il22*, normalized to that of the *18s*  
 15 gene, in Ctrl ( $n = 7$ ), Alc ( $n = 8$ ), Alc F<sub>3</sub> ( $n = 4$ ), Alc F<sub>3</sub> P2 ( $n = 15$ ), and Alc F<sub>3</sub> P6.5 ( $n = 16$ )  
 16 mice. (c-g) DMSO or Ficiz, mice treated with DMSO or Ficiz. (c) Liver *cyp1a1* and *scd1*,  
 17 normalized to that of the *gapdh* gene. (d) ALT level and liver triglyceride quantification in Ctrl  
 18 DMSO ( $n = 7$ ), Alc DMSO ( $n = 12$ ), Ctrl Ficiz ( $n = 8$ ), and Alc Ficiz ( $n = 8$ ) mice. (e) Liver  
 19 mRNA levels determined by qPCR: *ccl2* and *tnfa*, normalized to that of the *gapdh* gene, in Ctrl  
 20 DMSO ( $n = 6$ ), Alc DMSO ( $n = 11$ ), Ctrl Ficiz ( $n = 8$ ), and Alc Ficiz ( $n = 7$ ) mice. (f) Colon  
 21 mRNA levels determined by qPCR: *reg3β* and *reg3γ*, normalized to that of the *gapdh* gene. (g)  
 22 Ileum mRNA levels determined by qPCR: *reg3β* and *reg3γ*, normalized to that of the *gapdh*  
 23 gene, in Ctrl DMSO ( $n = 8$ ), Alc DMSO ( $n = 12$ ), Ctrl Ficiz ( $n = 8$ ), and Alc Ficiz ( $n = 10$ ) mice.

24

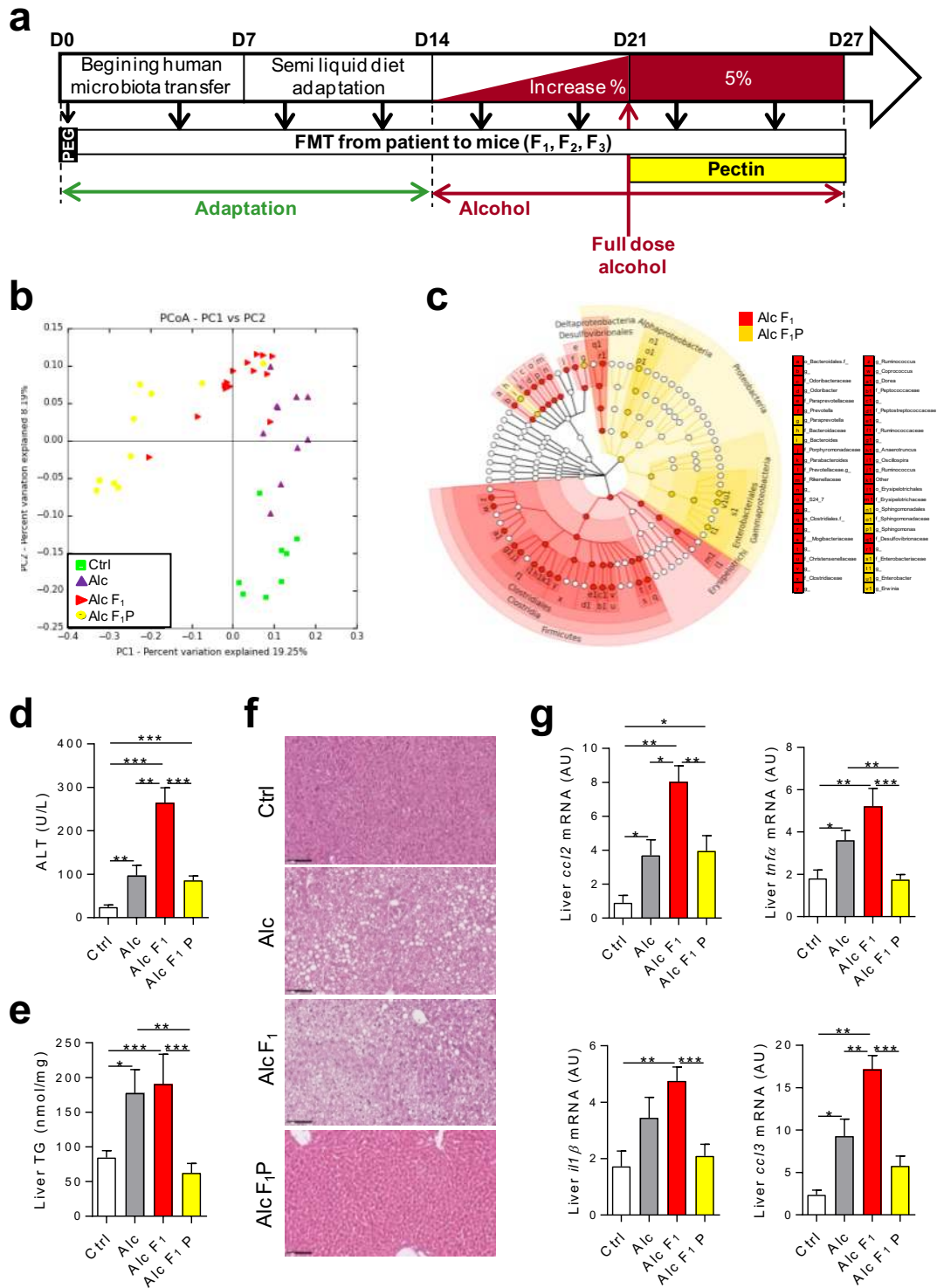
25 **Figure 4. KO of AhR partly blocks the liver protective effects of pectin.**

26 (a-d) WT, wild type mice; AhR KO, AhR deficient mice; Alc P2, alcohol-fed mice treated with  
 27 2% pectin. (a) ALT levels and liver triglyceride quantification in WT Ctrl ( $n = 8$ ), WT Alc ( $n$   
 28  $= 5$ ), WT Alc P ( $n = 8$ ), AhR KO Ctrl ( $n = 4$ ), AhR KO Alc ( $n = 4$ ), and AhR KO Alc P ( $n = 5$ )  
 29 mice. (b) Representative images of liver sections stained with hematoxylin-eosin, scale bar 100  
 30  $\mu\text{m}$ . (c,d) Colon mRNA levels determined by qPCR: *cyp1a1*, *ahr*, *il22*, *reg3β* and *reg3γ*,  
 31 normalized to that of the *18s* gene, in WT Ctrl ( $n = 8$ ), WT Alc ( $n = 5$ ), WT Alc P ( $n = 8$ ), AhR  
 32 KO Ctrl ( $n = 4$ ), AhR KO Alc ( $n = 4$ ), and AhR KO Alc P ( $n = 5$ ) mice. Results are shown as  
 33 the mean  $\pm$  SEM. Significant results for \* $p < 0.05$ , \*\* $p < 0.01$ , and \*\*\* $p < 0.001$  were  
 34 determined by Mann-Whitney tests unless stated otherwise.

1  
2  
3  
4  
5  
6  
7  
8

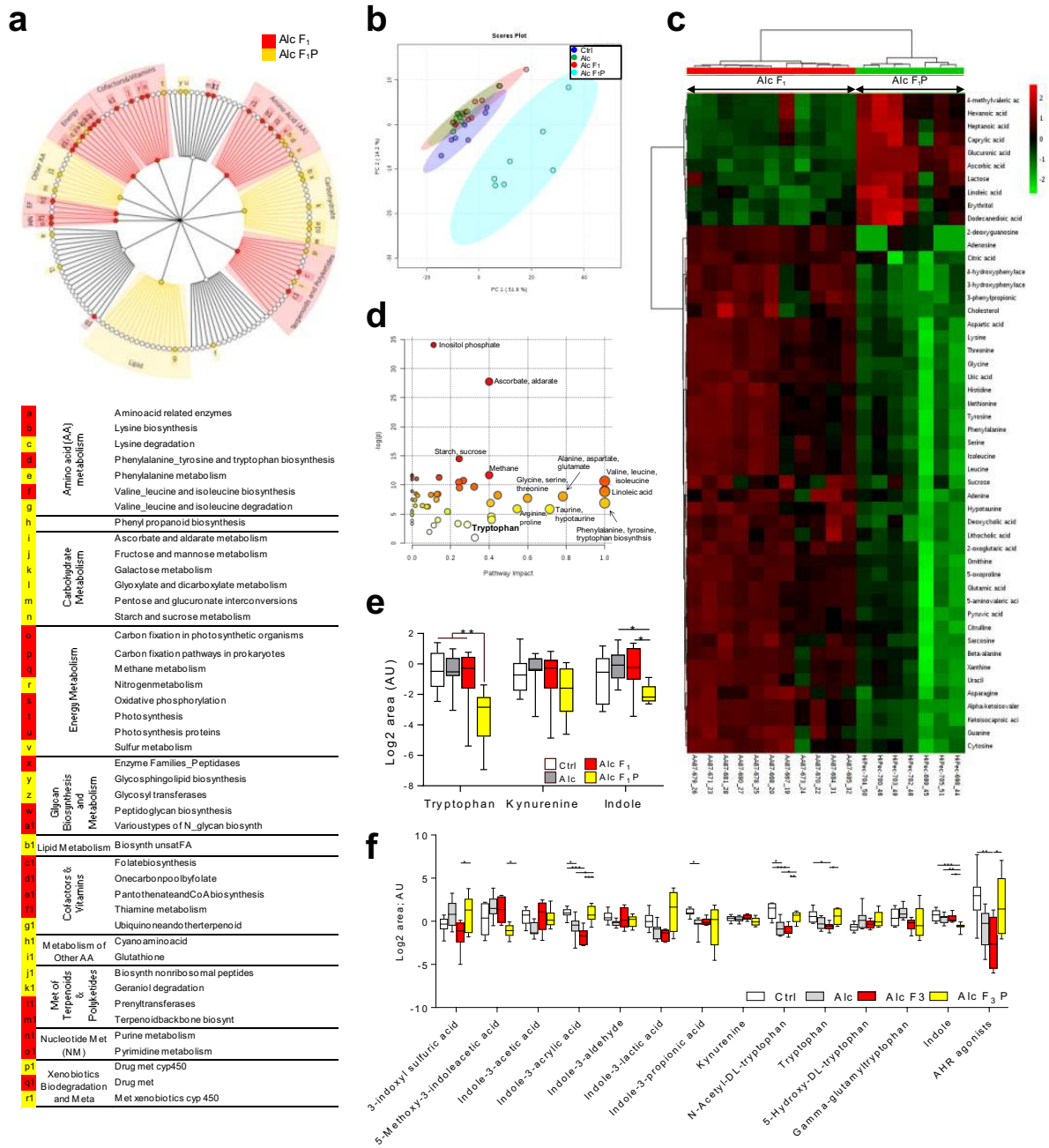
**Figure 5. Tryptophan metabolism is reduced in patients with severe alcoholic hepatitis (sAH) and correlates with disease severity. (a)** Serum concentrations of tryptophan, kynurenine, and AHR agonists (tryptamine, indole, indole 3-acetic acid, indole 3-acetaldehyde, and indoxyl sulfate) in sAH patients (n = 14) and patients without severe alcoholic hepatitis (noAH, n = 15). **(b)** Spearman correlation of the serum tryptophan and AST, bilirubin, and prothrombin time levels and MELD score.

Figure 1



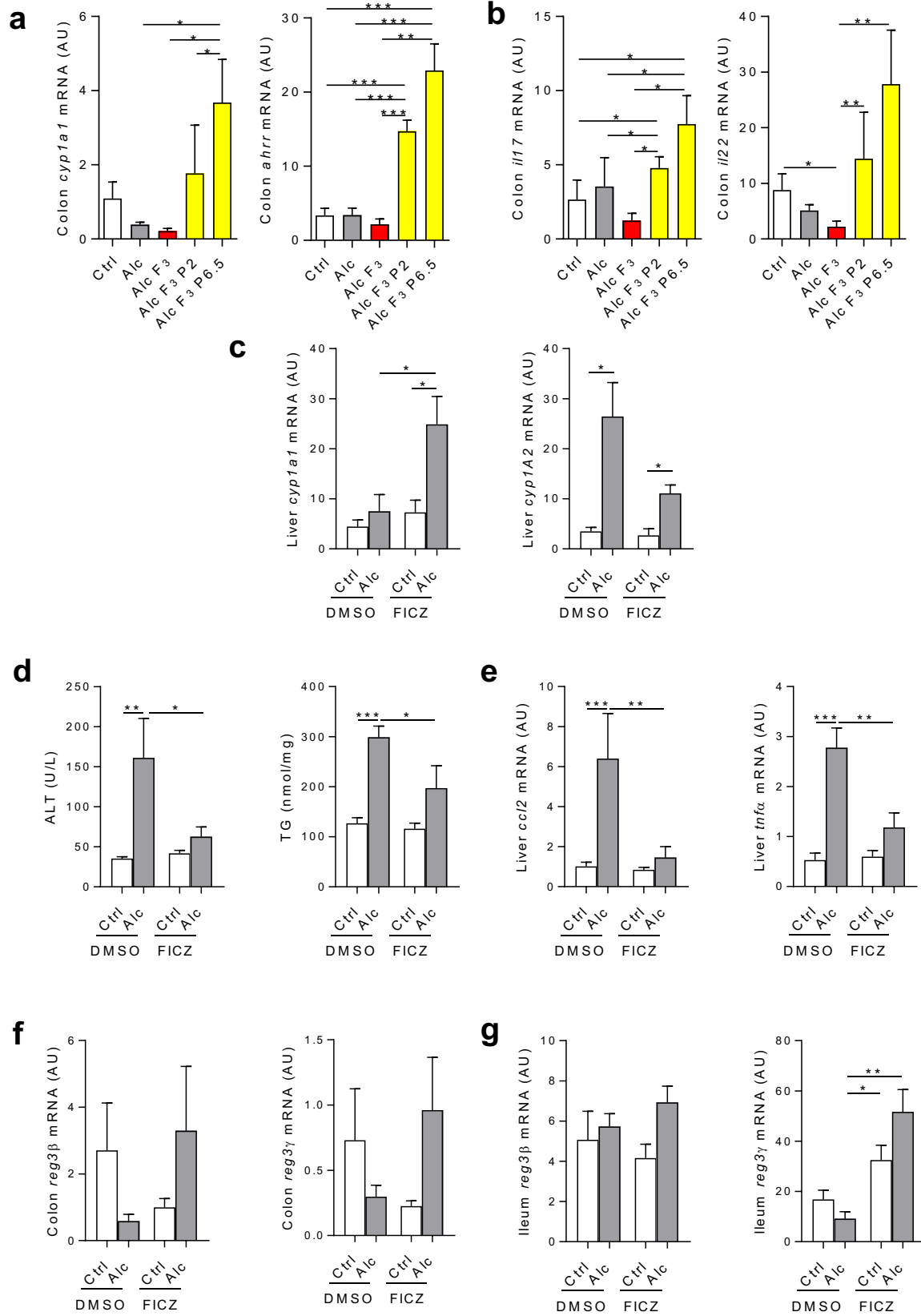
1  
2

Figure 2



1  
2

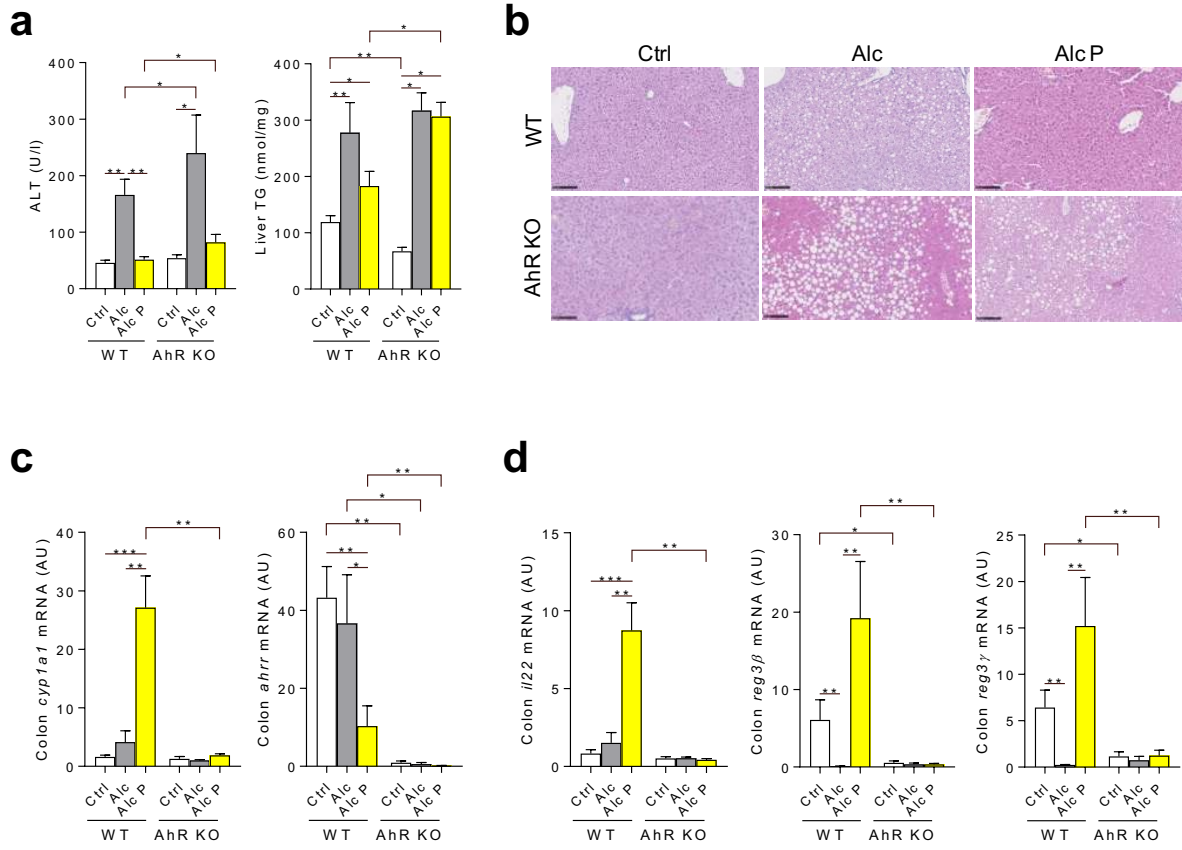
**Figure 3**



1

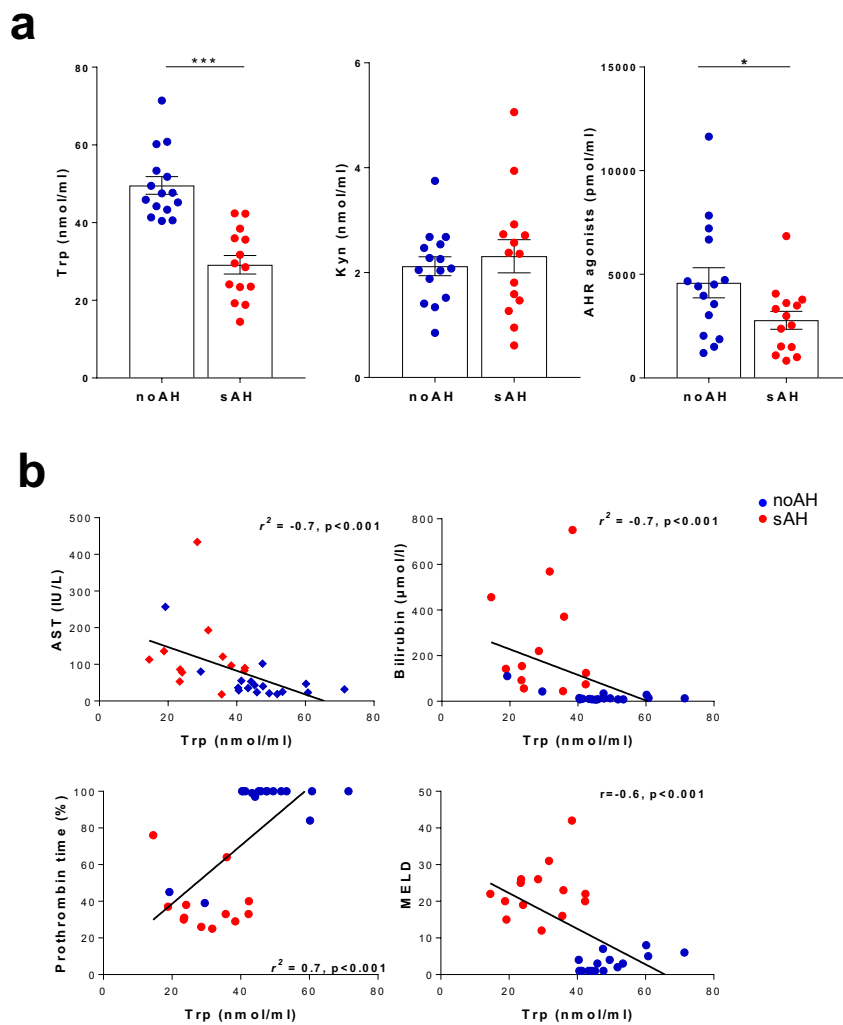
2

**Figure 4**



1  
2

## Figure 5



1

2

1		<b>SUPPLEMENTARY DATA</b>
2		
3		
4	<b>Material and methods</b>	<b>4</b>
5	<b>Supplementary Figure 1</b>	<b>10</b>
6	<b>Supplementary Figure 2</b>	<b>11</b>
7	<b>Supplementary Figure 3</b>	<b>12</b>
8	<b>Supplementary Figure 4</b>	<b>13</b>
9	<b>Supplementary Figure 5</b>	<b>14</b>
10	<b>Supplementary Figure 6</b>	<b>15</b>
11	<b>Supplementary Figure 7</b>	<b>16</b>
12	<b>Supplementary Figure 8</b>	<b>17</b>
13	<b>Supplementary Table 1</b>	<b>18</b>
14	<b>Supplementary Table 2</b>	<b>19</b>
15	<b>Supplementary Table 3</b>	<b>22</b>
16	<b>Supplementary Table 4</b>	<b>24</b>
17	<b>Supplementary Table 5</b>	<b>25</b>
18		



## 1 MATERIAL AND METHODS

2

3 ***Chronic exposure to alcohol.*** Eight-week old mice were fed a liquid diet adapted from Lieber  
4 DeCarli for 21 days, as previously described based on the NIAAA model<sup>3</sup> but without a binge  
5 administration of alcohol at the end. Briefly, the ethanol diet was obtained by adding absolute  
6 ethanol to a solution of Lieber DeCarli powder (Ssniff, Spezialdiäten GmbH, Soest, Germany)  
7 in filtered water. After a 7-day period of adaptation to the animal facility and a 7-day period  
8 adaptation to the semi-liquid diet, mice were given increasing amounts of ethanol for 7 days  
9 (1% increase every two days). The final concentration of ethanol in this liquid diet was 5%  
10 (vol/vol), such that ethanol accounted for 28% of the total caloric intake. The control diet was  
11 obtained by replacing the ethanol with an isocaloric amount of maltodextrin (Maldex 170, Safe,  
12 France). Alcohol-fed groups were allowed free access to the 5% (vol/vol) ethanol diet for 7  
13 days. Control mice were fed the isocaloric control diet throughout the entire feeding period.  
14 During the Lieber DeCarli diet, animals did not have access to drinking water. Diet  
15 consumptions were recorded and were similar between the groups (data not shown).

16

17 ***Tissues and samples.*** Mice were anesthetized and blood samples collected in EDTA coated  
18 tubes. Liver and distal colon were excised: one piece was fixed in buffered formaldehyde and  
19 another piece was snap-frozen in liquid nitrogen for TG and RNA extractions. All samples were  
20 stored at -80°C until use. Fecal samples were collected from mice immediately before  
21 euthanasia.

22

23 ***Measurement of bacterial translocation in the liver.*** Liver were collected in sterile conditions  
24 and disrupted in 2 ml of PBS 1X. 500 µl of lysate were put on PolyVitex chocolate agar  
25 (Biomérieux, Capronne, France), spread with balk and place in incubator in anaerobic  
26 conditions at 37°C during 48 to 72 hours and colony-forming unit were counted.

27

28 ***Measurement of liver triglycerides and blood samples.*** Liver triglycerides were extracted using  
29 a triglyceride quantification kit following the manufacturer's indications (Abcam, Cambridge,  
30 UK). Quantification was performed by using a Berthold Technologies colorimetric microplate  
31 reader (Mithras LB 940), and the level of liver TG was expressed in nmol per milligram of liver.  
32 Plasma alanine aminotransferase (ALT), aspartate transaminase (AST), triglycerides, high-  
33 density lipoprotein (HDL) and cholesterol levels were assed using a spectrophotometric method

1 (Olympus, AU400). Alcohol was measured in the plasma by using the colorimetric assay kit  
2 (Biovision).

3

4 ***Liver and gut histology.*** Liver and gut (colon) were fixed overnight in 4% paraformaldehyde  
5 and embedded in paraffin. Paraffin sections (4  $\mu\text{m}$  thick) were stained with hematoxylin and  
6 eosin (H&E). Colon samples were also stained with Alcian Blue.

7

8 ***Immunofluorescence.*** Specimens were embedded in paraffin and cut in 3- $\mu\text{m}$  section. Staining  
9 with antibodies purchased from abcam against ZO-1 (ab96587) and occludine (ab216327) was  
10 done, followed by staining with a fluorochrome-coupled secondary antibody goat anti-rabbit  
11 Alexa Fluor™ Plus 594 (Invitrogen, Thermo Fisher Scientific). Nuclei were stained with  
12 Hoechst (Life Technologies, Thermo Fisher Scientific). Slides were scanned by the digital slide  
13 scanner NanoZoomer 2.0-RS (Hamamatsu, France) allowing an overall view of the samples.  
14 Images were digitally captured from the scanned slides using the NDP.view2 software  
15 (Hamamatsu, France).

16

17 ***RNA extraction and quantification.*** Mice livers were disrupted in Qiazol solution. Total RNA  
18 was extracted using a Qiagen RNeasy Lipid tissue minikit (Courtaboeuf, France). Total gut  
19 RNA was extracted using a Qiagen RNeasy Plus Mini Kit (Courtaboeuf, France), after being  
20 disrupted with an MP Biomedicals FastPrep. The RNA integrity number (RIN) was determined  
21 using an Agilent Bioanalyzer 2100 system with the RNA 6000 Nano Labchip kit. Samples with  
22 a RIN of less than 8 were eliminated. For cDNA synthesis, 1  $\mu\text{g}$  of each total RNA sample was  
23 reverse transcribed. A 12  $\mu\text{l}$  mix containing 1  $\mu\text{g}$  of RNA, random hexamers (Roche  
24 Diagnostics, Meylan, France), and 10 mM dNTP Mix (Invitrogen, Carlsbad, CA) was prepared  
25 for each sample. Mixtures were heated at 65°C for 5 min, cooled on ice, and then an 8  $\mu\text{l}$  reaction  
26 mix containing 1  $\mu\text{l}$  M-MuL<sub>v</sub> RT (Invitrogen), 4  $\mu\text{l}$  5x Buffer (Invitrogen), 2  $\mu\text{l}$  0.1 M  
27 dithiothreitol (Invitrogen), and 1  $\mu\text{l}$  Protector RNase Inhibitor (40 U/ $\mu\text{l}$ ; Invitrogen) was added.  
28 The reaction conditions were 10 min at 25°C, 50 min at 50°C, 15 min at 70°C.

29

30 ***Gene expression analysis by quantitative qPCR.*** Real-time qPCR was performed in a Light  
31 Cycler 480 (Roche Diagnostics) using the LC FastStart DNA Master SYBR Green I kit (Roche  
32 Diagnostics). Amplification was initiated with an enzyme activation step at 95°C for 10 min,  
33 followed by 40 cycles consisting of a 20 s denaturation step at 95°C, a 15 s annealing step at  
34 the temperature appropriate for each primer, and a 45 s elongation step at 72°C. We amplified

1 the cDNAs for *18s*, *gapdh*, *tnfa*, *tgfb*, *il1b*, *ccl2*, *ccl3*, *reg3b*, *reg3g*, *il22*, *il17*, *ahrr* and *cyp1a1*.  
2 Primer sequences are listed in Supplemental Table 5. Data were analyzed using Light Cycler  
3 480 Software (Roche Diagnostics). Relative gene expression was normalized to the *18s* or  
4 *gapdh* reference gene.

5

6 ***Analysis of the intestinal microbiota by 16S RNA sequencing.*** The composition of the  
7 microbiota was analyzed using Illumina MiSeq technology targeting the 16S ribosomal DNA  
8 V3-V4 region in paired-end modus (2 x 300 base pair) (GenoToul, Toulouse). Bacterial DNA  
9 was obtained by homogenizing stools in a Guanidinium thiocyanate containing lysis buffer  
10 using a Fast Prep homogenizer. High quality bacterial DNA was extracted by successive steps  
11 of purification and precipitation using “Laboratory-made” buffers <sup>4</sup>. PCR were performed to  
12 prepare amplicons using V3-V4 oligonucleotides (PCR1F\_460: 5’  
13 CTTTCCCTACACGACGCTCTTCCGATCTACGGRAGGCAGCAG 3’, PCR1R\_460: 5’  
14 GGAGTTCAGACGTGTGCTCTTCCGATCTTACCAGGGTATCTAATCCT 3’). Amplicon  
15 quality was verified by gel electrophoresis and they were sent to the GenoToul platform for  
16 sequencing. The resulting paired reads were assembled using PANDAseq v 2.7 to generate an  
17 amplicon size of 450 base pairs <sup>5</sup>. Reads were demultiplexed and processed using the  
18 quantitative insights into microbial ecology (QIIME v1.9.0) pipeline and the default parameters  
19 of QIIME<sup>6</sup>. Chimeric sequences were identified *de novo*, reference based, and then removed  
20 using usearch61 <sup>7</sup>. The non-chimeric sequences were then clustered into operational taxonomic  
21 units (OTUs) at 97.0% sequence similarity using a closed reference-based picking approach  
22 with UCLUST software against the Greengenes database 13\_8 of bacterial 16S rDNA  
23 sequences <sup>8</sup>. The mean number of quality-controlled reads was 25034 ± 6875 (mean ± SD) per  
24 sample. After rarefaction at 7,000 reads per sample, bacterial alpha diversity was estimated  
25 using Shannon index. OTUs with a prevalence < 5% were removed from the analysis. Analyses  
26 using R software v2.14.1 were restricted to merged OTUs with the same taxonomic assignment.  
27 Results are represented as the mean ± SEM. The Wilcoxon test was used to assess statistical  
28 significance of the bacterial composition between the different samples. Associations were  
29 considered to be significant after a false-discovery rate (FDR) correction of the p-value (q <  
30 0.05).

31 Beta diversity was assessed using weighted and unweighted UniFrac distances. The weighted  
32 Unifrac metric is weighted by the difference in the abundance of OTUs from each community,  
33 whereas unweighted Unifrac only considers the absence/presence of the OTUs providing  
34 different information. The link between the different groups of mice and bacterial microbial

1 profiles was addressed by performing an ANOSIM test with 10,000 permutations on the beta  
2 diversity metrics described above.

3 Functional composition of the intestinal metagenome was predicted using Phylogenetic  
4 Investigation of Communities by Reconstruction of Unobserved States (PICRUSt) <sup>9</sup>. This is a  
5 computational approach that accurately predicts the abundance of gene families in the  
6 microbiota and thus provides information about the functional composition of the microbial  
7 community. Linear discriminant analysis (LDA) effect size (LEfSe) analysis was performed to  
8 identify the taxa and functions displaying the largest differences in abundance in the microbiota  
9 between groups <sup>10</sup>. Only taxa and functions with an LDA score > 2 and a significance of < 0.05,  
10 as determined by Wilcoxon signed-rank tests, are shown. LEfSe and PICRUSt were accessed  
11 online (<http://huttenhower.sph.harvard.edu/galaxy/>).

12

13 ***Analysis of fecal metabolites by gas chromatography coupled to a triple quadrupole mass***  
14 ***spectrometer.*** Fecal metabolites were measured using the GC-MS/MS method as previously  
15 described <sup>11</sup>. Briefly, about 20 mg of biological material for each sample were first weighted  
16 and solubilized into microcentrifuge tubes with 500 µL of MilliQ water (+4°C). Samples were  
17 snap frozen in liquid nitrogen, then thaw at room temperature on the bench, while they were  
18 thoroughly vortex. Samples were splitted in two parts: the first 200 µl were added to 300 µl of  
19 cold methanol, the others 200 µl were added to 300 µl of cold TBME. The two aliquots were  
20 centrifugated 10 minutes at 15000g (+4 °C). Concerning the TBME extraction, the upper layer  
21 was transferred in vial for direct injection into Gas Chromatography coupled with Mass  
22 Spectrometry (GC/MS, WAX method). Concerning the methanol extraction, 400 µl of the  
23 supernatant were transferred and evaporated in microcentrifuge tubes at 40°C in a  
24 pneumatically assisted concentrator (Techne DB3, Staffordshire, UK). On dried extract, 300 µl  
25 of methanol were added then splitted in two aliquots: the first 150 µL used for GC/MS (HP5MS  
26 method) experiment in vial injection, the others 150 µL used for the Ultra High Pressure Liquid  
27 Chromatography coupled by Mass Spectrometry (UHPLC/MS) experimentations. Concerning  
28 the GC/MS (HP5MS) aliquots, the 150 µL were evaporated and 50 µL of methoxyamine (20  
29 mg/mL in pyridine) was added on dried extracts, and stored at room temperature in dark, during  
30 16 hours. The day after, 80 µL of MSTFA was added and final derivatization occurred at 40°C  
31 during 30 minutes. Samples were then directly injected into GC-MS.

32 Concerning the LC-MS aliquots, the collected supernatant was evaporated in microcentrifuge  
33 tubes at 40°C in a pneumatically assisted concentrator (Techne DB3, Staffordshire, UK). The  
34 LC-MS dried extracts were solubilized with 450 µL of MilliQ water and aliquoted in 3

1 microcentrifuge tubes (100  $\mu$ L) for each LC method and one microcentrifuge tube for backup.  
2 Aliquots for analysis were transferred in LC vials and injected into UHPLC/MS or kept at -  
3 80°C until injection.

4 The GC-MS/MS method was performed on a 7890B gas chromatography (Agilent  
5 Technologies, Waldbronn, Germany) coupled to a triple quadrupole 7000C (Agilent  
6 Technologies, Waldbronn, Germany) equipped with a High sensitivity electronic impact source  
7 (EI) operating in positive mode.

8 The front inlet temperature was 250°C, the injection was performed in splitless mode. The  
9 transfer line and the ion-source temperature were 250°C and 230°C, respectively. The septum  
10 purge flow was fixed at 3 mL/min, the purge flow to split vent operated at 80 mL/min during 1  
11 min and gas saver mode was set to 15 mL/min after 5 min.

12 The helium gas flowed through the column (J&WScientificHP-5MS, 30m x 0.25 mm, i.d. 0.25  
13 mm, d.f., Agilent Technologies Inc.) at 1 mL/min. Column temperature was held at 60°C for 1  
14 min, then raised to 210°C (10°C/min), followed by a step to 230°C (5°C/min) and reached  
15 325°C (15°C/min), and be hold at this temperature for 5 min.

16 The scan mode used was the MRM for biological samples. Peak detection and integration of  
17 the analytes were performed using the Agilent Mass Hunter quantitative software (B.07.01).

18 All the statistical analysis and pathway annotations for the metabolites were carried out using  
19 MetaboAnalyst web tool ([www.metaboanalyst.ca](http://www.metaboanalyst.ca))<sup>12</sup>. Data was normalized using log  
20 transformation and Pareto-scaling. For multi group analysis, one-way ANOVA was performed  
21 followed by post-hoc analyses using Tukey's HSD. For predicting variance in samples,  
22 Principal Component Analysis (PCA) was performed. The significant pathways involved in the  
23 pectin effect were also identified using MetaboAnalyst tool<sup>13</sup>.

24

25 ***Measurement of tryptophan metabolites in the feces and plasma of patients.*** Indole derivatives  
26 were quantified HPLC-coupled to high resolution mass spectrometry as previously described  
27 <sup>14</sup>.

28

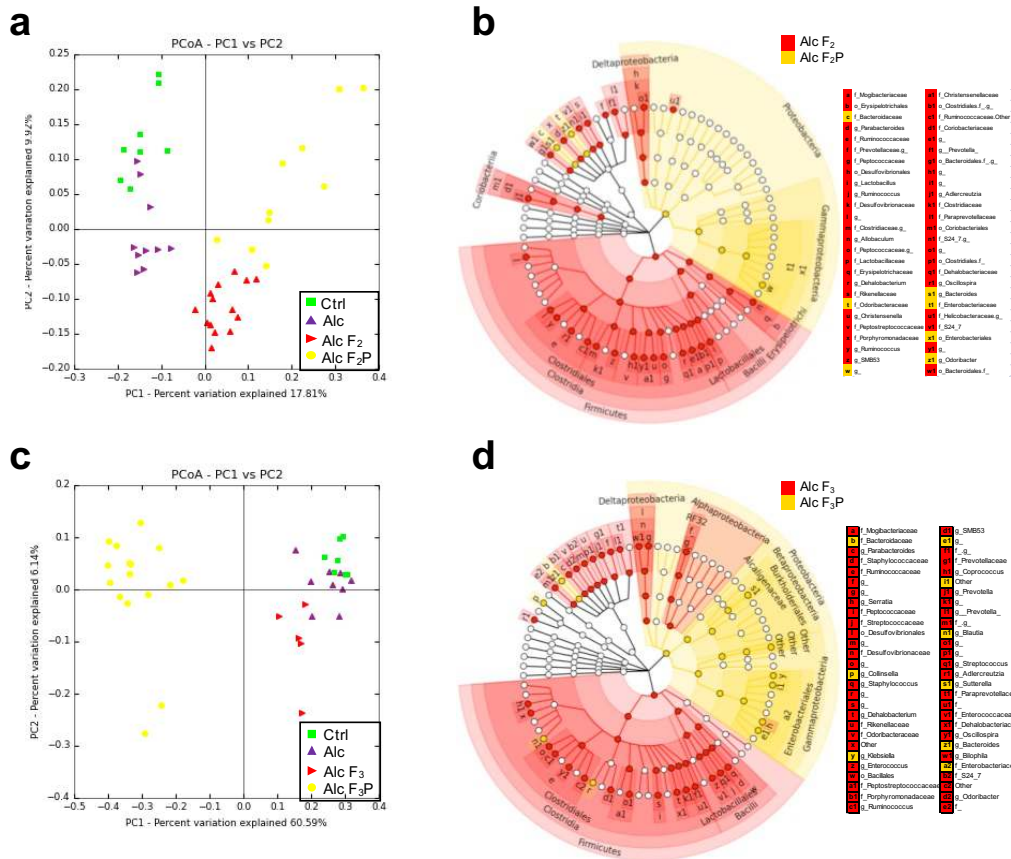
29

## 30 REFERENCES

- 31 1-Llopis M, et al. (2016) *Gut* 65(5):830-839.  
32 2-Wrzosek L, et al. (2018) *Sci Rep* 8(1):6854.  
33 3-Bertola A, et al. (2013) *Nature protocols* 8(3):627-637.  
34 4-Tomas J, et al. (2013) *FASEB J.* 27(2):645-655.  
35 5-Masella AP, et al. (2012) *BMC Bioinformatics* 13:31.

- 1 **6**-Caporaso JG, *et al.* (2010) *Nat Methods* 7(5):335-336.
- 2 **7**-Edgar RC (2010) *Bioinformatics* 26(19):2460-2461.
- 3 **8**-DeSantis TZ, *et al.* (2006) *Appl. Environ. Microbiol.* 72(7):5069-5072.
- 4 **9**-Langille MG, *et al.* (2013) *Nat. Biotechnol.* 31(9):814-821.
- 5 **10**-Segata N, *et al.* (2011) *Genome Biol* 12(6):R60.
- 6 **11**-Pietrocola F, *et al.* (2017) *Autophagy* 13(12):2163-2170.
- 7 **12**-Chong J, *et al.* (2018) *Nucleic Acids Res* 46(W1):W486-W494.
- 8 **13**-Xia J, *et al.* (2016) *Curr Protoc Bioinformatics* 55:14 10 11-14 10 91.
- 9 **14**-Lefevre A, *et al.* (2019) *Talanta* 195:593-598.
- 10

## Supplementary Figure 1



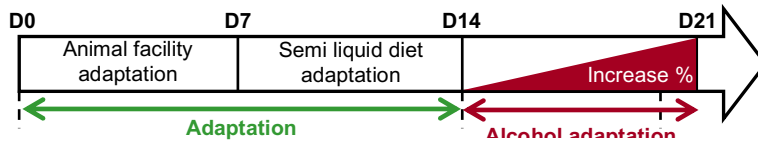
**Supplementary Figure 1. The composition of the intestinal microbiota of mice humanized with feces from two patients with severe alcoholic hepatitis is modified by pectin treatment.** Ctrl, control-fed mice; Alc, alcohol-fed mice; Alc F2 and Alc F3, alcohol-fed mice humanized with the microbiota from a patient with sAH (patient F2 or F3); Alc F2 P6.5 and Alc F3 P6.5, alcohol-fed mice humanized with the microbiota from a patient with sAH (patient F2 or F3) and treated with 6.5% pectin. (a) Principal Coordinate Analysis (PCoA) plot showing the unweighted UniFrac distance ( $p < 0.001$ ,  $R = 0.59$ , ANOSIM test, 10,000 permutations, using the first 5 PC). (b) Cladograms showing the taxa most differentially associated with Alc F2 (red) or Alc F2 P6.5 mice (yellow) (Wilcoxon rank-sum test). Circle sizes in the cladogram plot are proportional to bacterial abundance. The circles represent, going from the inner to outer circle: phyla, genus, class, order, and family. Mice per group for **a** and **b**: Ctrl ( $n=8$ ), Alc ( $n=10$ ), Alc F2 ( $n=15$ ), and Alc F2 P6.5 ( $n=10$ ). (c) PCoA plot showing the unweighted UniFrac distance ( $p < 0.001$ ,  $R = 0.68$ , ANOSIM test, 10,000 permutations, using the first 5 PC). (d) Cladograms showing the taxa most differentially associated with Alc F3 (red) or Alc F3 P6.5 mice (yellow) (Wilcoxon rank-sum test). Mice per group in **c** and **d**: Ctrl ( $n=9$ ), Alc ( $n=9$ ), Alc F3 ( $n=5$ ), Alc F3 P0.4 ( $n=8$ ), Alc F3 P1 ( $n=11$ ), Alc F3 P2 ( $n=16$ ), and Alc F3 P6.5 ( $n=16$ ).

1  
2

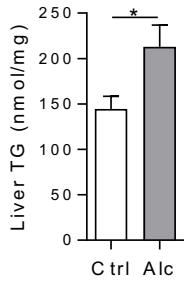
## Supplementary Figure 2

1

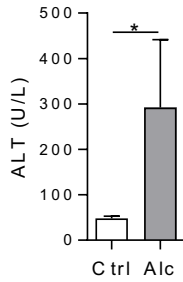
2 a



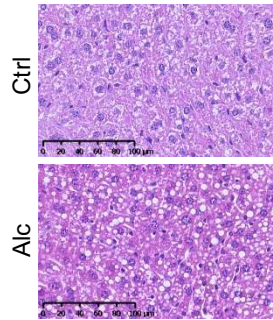
b



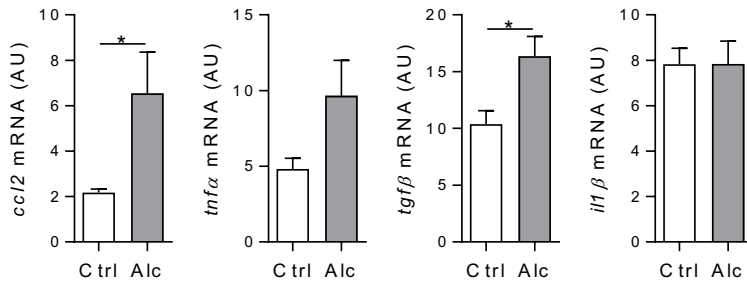
c



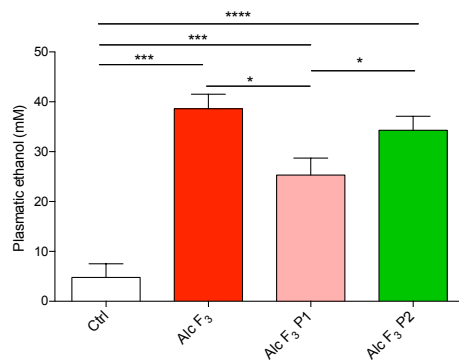
d



e



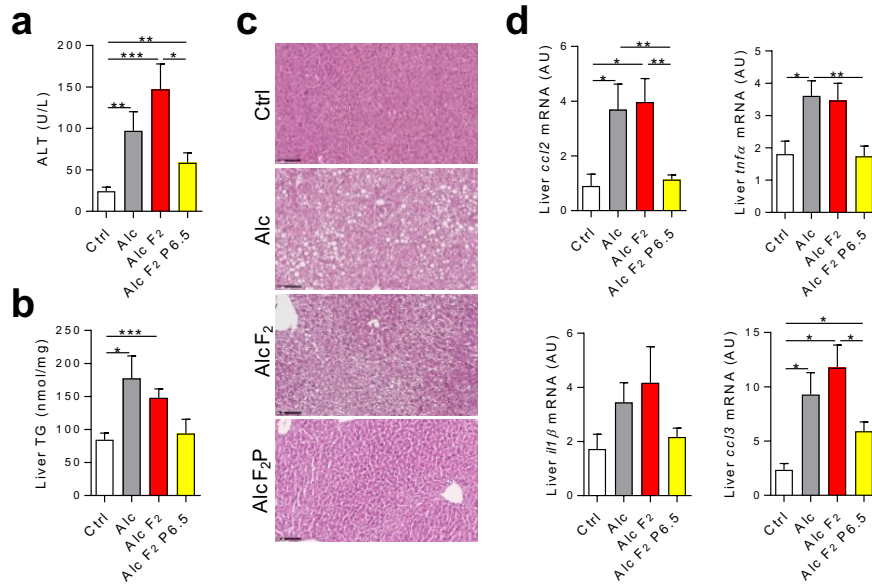
f



**Supplementary Figure 2. Alcohol-induced liver injury after the alcohol adaptation period.** Ctrl, control-fed mice (n=11); Alc, alcohol-fed mice (n=11). (a) Experimental design: mice were progressively adapted to a semi-liquid, Lieber DeCarli (LDC) diet, then to an ethanol diet, using increasing doses of ethanol (2-4%) for seven days. (b) ALT level. (c) Liver triglyceride quantification. (d) Representative pictures of liver sections stained with haematoxylin-eosin in control and alcohol-fed mice showing steatosis, scale bar 100  $\mu$ m. (e) Liver mRNA levels of inflammation markers were determined by qPCR: *ccl2*, *tnfa*, *tgfb*, and *il1b*, normalized to that of the *gapdh* gene. (f) Plasmatic alcohol in control mice (Ctrl) and alcohol fed mice transplanted with MI of sAH patient (Alc sAH) and treated with 1% or 2% of pectin. Results are shown as the mean  $\pm$  SEM. Significant results for \* $p < 0.05$ , \*\*\* $p < 0.0002$ , \*\*\*\* $p < 0.0001$  were determined by the Mann-Whitney test.



## Supplementary Figure 3

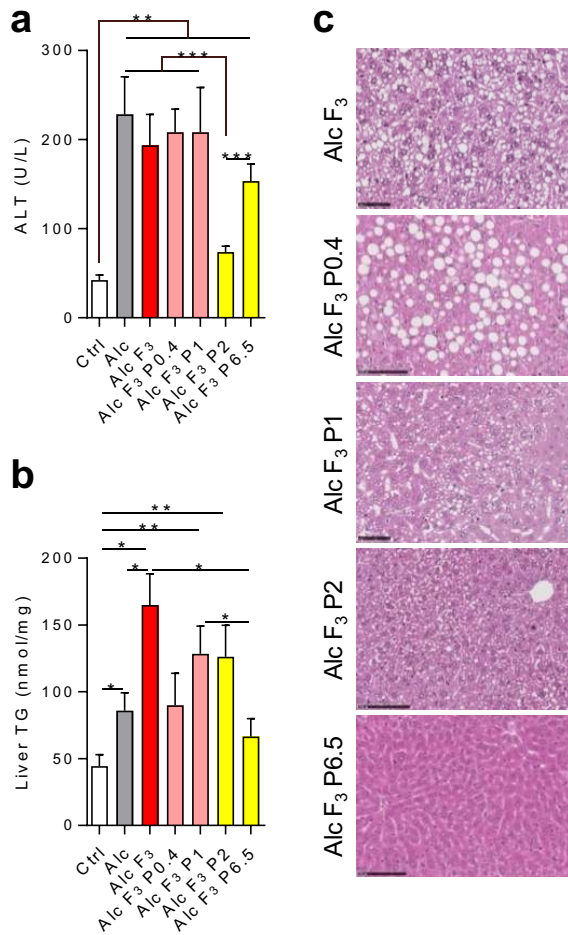


**Supplementary Figure 3. Pectin treatment reverses liver lesions in mice humanized with the intestinal microbiota from a patient with severe alcoholic hepatitis.** Ctrl, control-fed mice; Alc, alcohol-fed mice; Alc F2, alcohol-fed mice humanized with the microbiota from a patient with sAH (patient F2); Alc F2 P6.5, alcohol-fed mice humanized with the microbiota from a patient with sAH (patient F2) and treated with 6.5% pectin. **(a)** ALT level in Ctrl (n=8), Alc (n=8), Alc F2 (n=16), and Alc F2 P6.5 (n=10) mice. **(b)** Liver triglyceride quantification in Ctrl (n=8), Alc (n=8), Alc F2 (n=14), and Alc F2 P6.5 (n=8) mice. **(c)** Representative images of liver sections stained with haematoxylin-eosin, scale bar 100  $\mu$ m. **(d)** Liver mRNA levels determined by qPCR: *ccl2*, *tnfa*, *il1b* and *ccl3* normalized to that of the *gapdh* gene in Ctrl (n=4), Alc (n=5), Alc F2 (n=16), and Alc F2 P6.5 (n=9) mice. Results are shown as the mean  $\pm$  SEM. Significant results for \* $p < 0.05$ , \*\* $p < 0.01$ , and \*\*\* $p < 0.001$  were determined by Mann-Whitney tests unless stated otherwise.

1

2

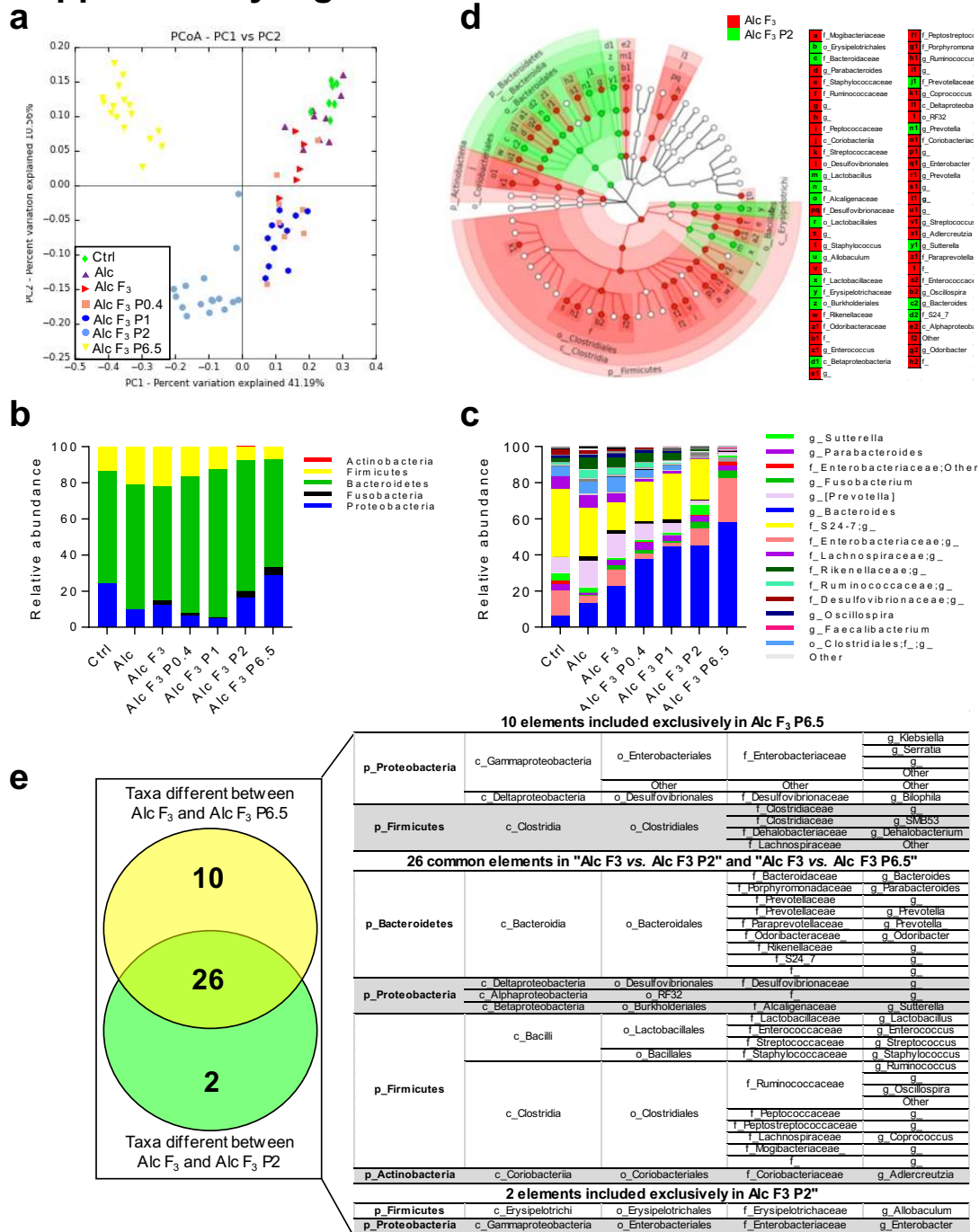
## Supplementary Figure 4



**Supplementary Figure 4. Dose-dependent effect of pectin on liver and intestinal barrier function.** Ctrl, control-fed mice; Alc, alcohol-fed mice; Alc F3, alcohol-fed mice humanized with the microbiota from a patient with sAH (patient F3); Alc F3 P0.4, Alc F3 P1, Alc F3 P2, and Alc F3 P6.5, alcohol-fed mice humanized with the microbiota from a patient with sAH (patient F3) and treated with 0.4, 1, 2, or 6.5% pectin, respectively. (a) ALT levels in Ctrl (n=8), Alc (n=9), Alc F3 (n=6), Alc F3 P0.4 (n=9), Alc F3 P1 (n=12), Alc F3 P2 (n=15), and Alc F3 P6.5 (n=16) mice. (b) Liver triglyceride quantification in Ctrl (n=8), Alc (n=9), Alc F3 (n=3), Alc F3 P0.4 (n=7), Alc F3 P1 (n=10), Alc F3 P2 (n=16), and Alc F3 P6.5 (n=14) mice. (c) Representative images of liver sections stained with haematoxylin-eosin, scale bar 400  $\mu$ m. Results are shown as the mean  $\pm$  SEM. Significant results for \* $p$  < 0.05, \*\* $p$  < 0.01, and \*\*\* $p$  < 0.001 were determined by Mann-Whitney tests unless stated otherwise.

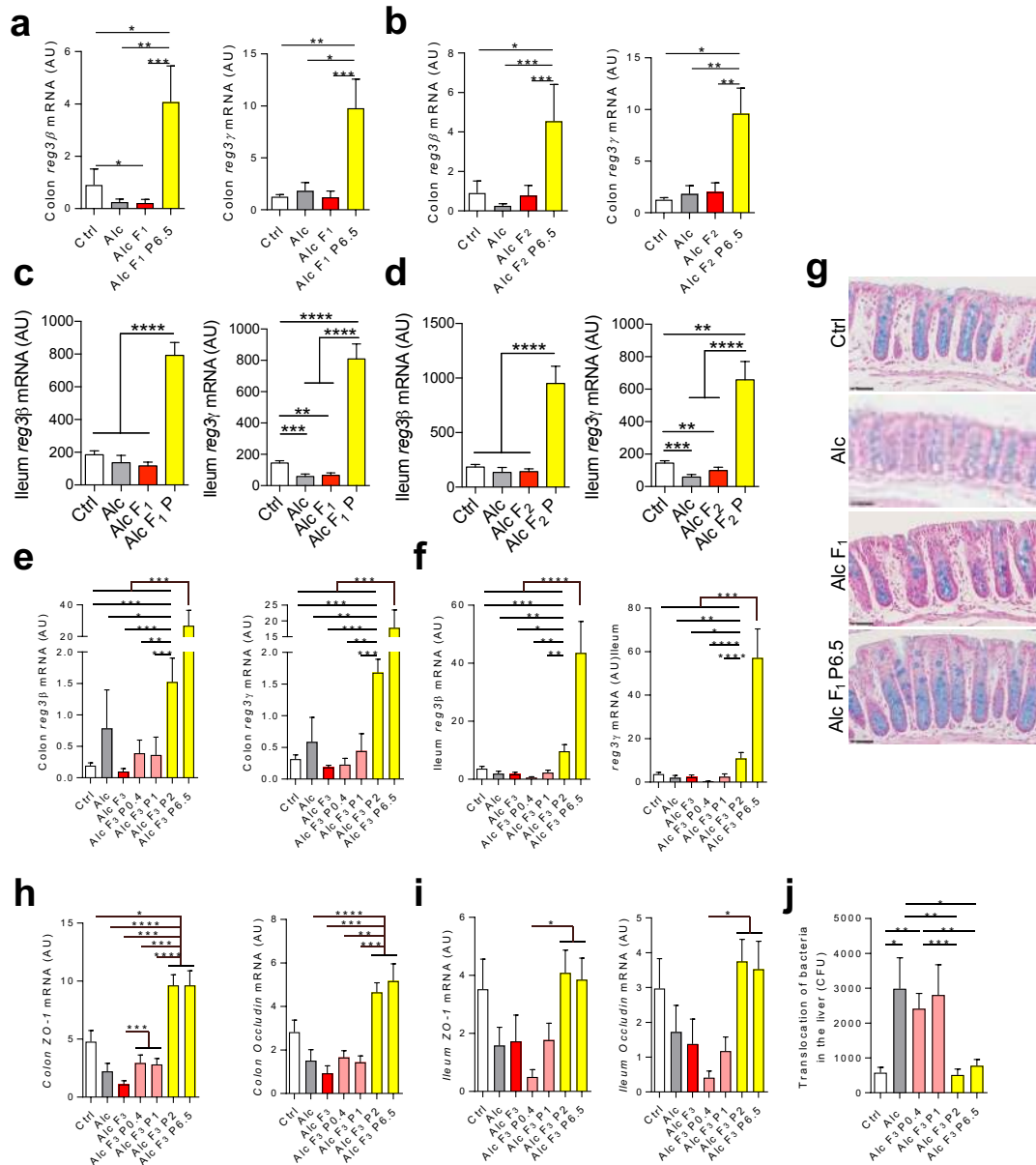
1  
2

### Supplementary Figure 5



**Supplementary Figure 5. Gut microbiota composition of mice humanized with intestinal microbiota from a patient with severe alcoholic and treated with different doses of pectin.** Alc, alcohol-fed mice (n=5); Ctrl, control-fed mice (n=7); Alc F<sub>3</sub> (n=5), alcohol-fed mice humanized with the microbiota from a patient with sAH (patient F<sub>3</sub>); Alc F<sub>3</sub> P0.4 (n=8), Alc F<sub>3</sub> P1 (n=11), Alc F<sub>3</sub> P2 (n=16), Alc F<sub>3</sub> P6.5 (n=16), alcohol-fed mice humanized with the microbiota from a patient with sAH (patient F<sub>3</sub>) and treated with pectin 0.4%, 1%, 2% or 6.5% respectively. (a) PCoA plot showing the unweighted UniFrac distance (p < 0.001, R= 0.75, ANOSIM test, 10,000 permutations, using the first 5 PC). (b) Bacterial taxon-based analysis at the phylum and (c) genus level in faecal microbiota (d) LDA effect size (LEfSe) cladograms showing the taxa most differentially associated with Alc F<sub>3</sub> (red) or Alc F<sub>3</sub> P2 mice (green) (Wilcoxon rank-sum test). Circle sizes in the cladogram plot are proportional to bacterial abundance. The circles represent, going from the inner circle to the outer circle: phyla, genus, class, order, and family. (e) Venn diagram based on the taxa different in LEfSe analysis between Alc F<sub>3</sub> vs. Alc F<sub>3</sub> P6.5 and Alc F<sub>3</sub> vs. Alc F<sub>3</sub> P2 and the corresponding common taxa between these two comparisons.

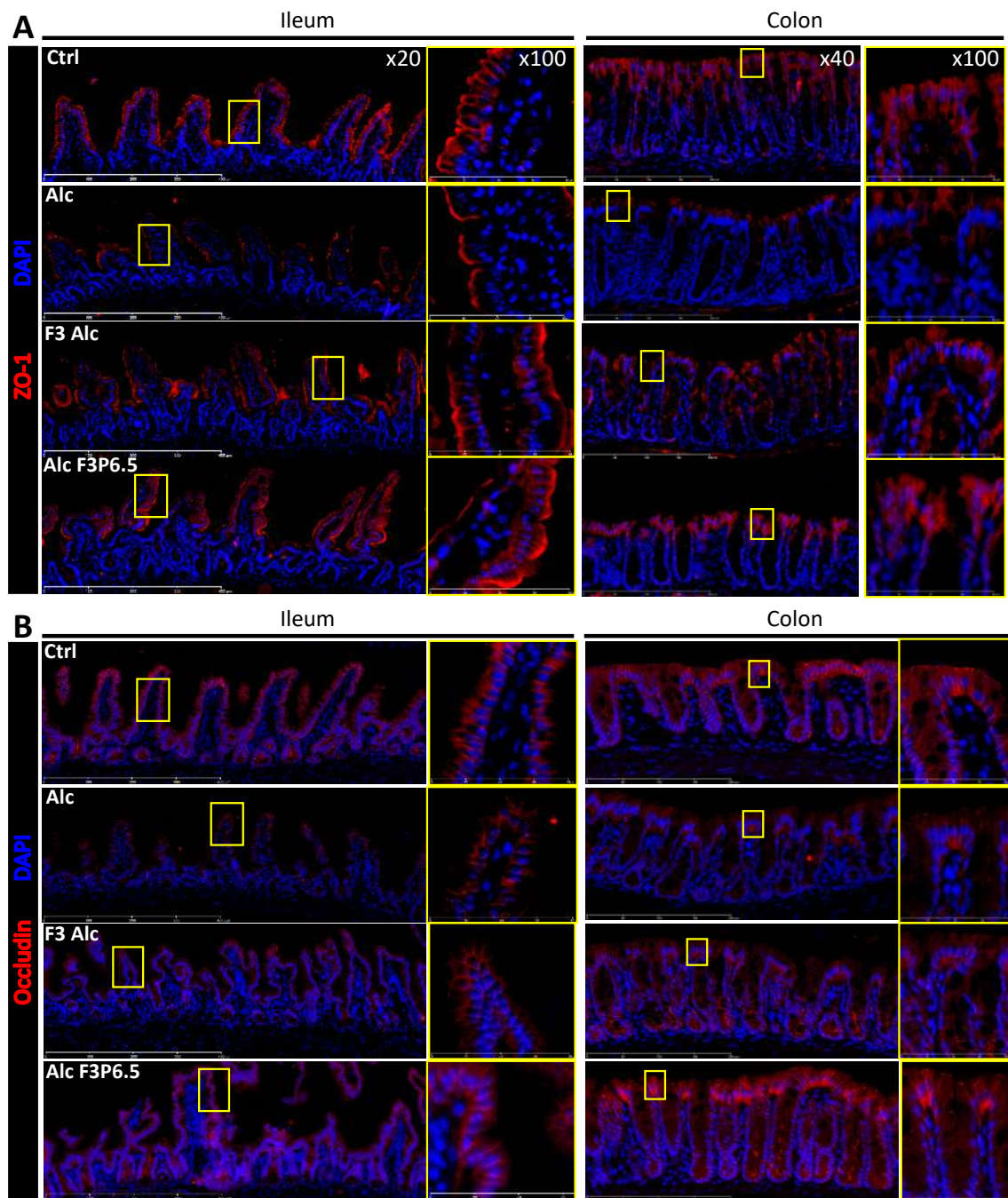
## Supplementary Figure 6



**Supplementary Figure 6. Pectin treatment improves intestinal barrier function.** Ctrl, control-fed mice; Alc, alcohol-fed mice; Alc F1, Alc F2 and Alc F3, alcohol-fed mice humanized with the microbiota from a patient with sAH (patients F1, F2 or F3); Alc F1 P6.5, Alc F2 P6.5 and Alc F3 P6.5, alcohol-fed mice humanized with the microbiota from a patient with sAH (patient 1, 2, or 3) and treated with 6.5% pectin. (a-f) Colon and ileum mRNA levels determined by qPCR: *reg3β* and *reg3γ* normalized to that of the *gapdh* gene. (e) Representative images of colon sections stained with Alcian blue, scale bar 50  $\mu$ m. (h) Colon and (i) ileum mRNA levels determined by qPCR: *ZO-1* and *occludin* normalized to that of the *18s* gene. (j) Culture of bacteria in the liver. For a-d and g: Ctrl (n=8), Alc (n=8), Alc F1 (n=12), Alc F1 P6.5 (n=10), Alc F2 (n=16) and Alc F2 P6.5 (n=10) mice. For e-j: Ctrl (n=8), Alc (n=9), Alc F3 P0.4 (n=9), Alc F3 P1 (n=12), Alc F3 P2 (n=13), and Alc F3 P6.5 (n=13) mice. Results are shown as the mean  $\pm$  SEM. Significant results for \*p < 0.05, \*\*p < 0.01, and \*\*\*p < 0.001 were determined by Mann-Whitney tests unless stated otherwise.

1  
2

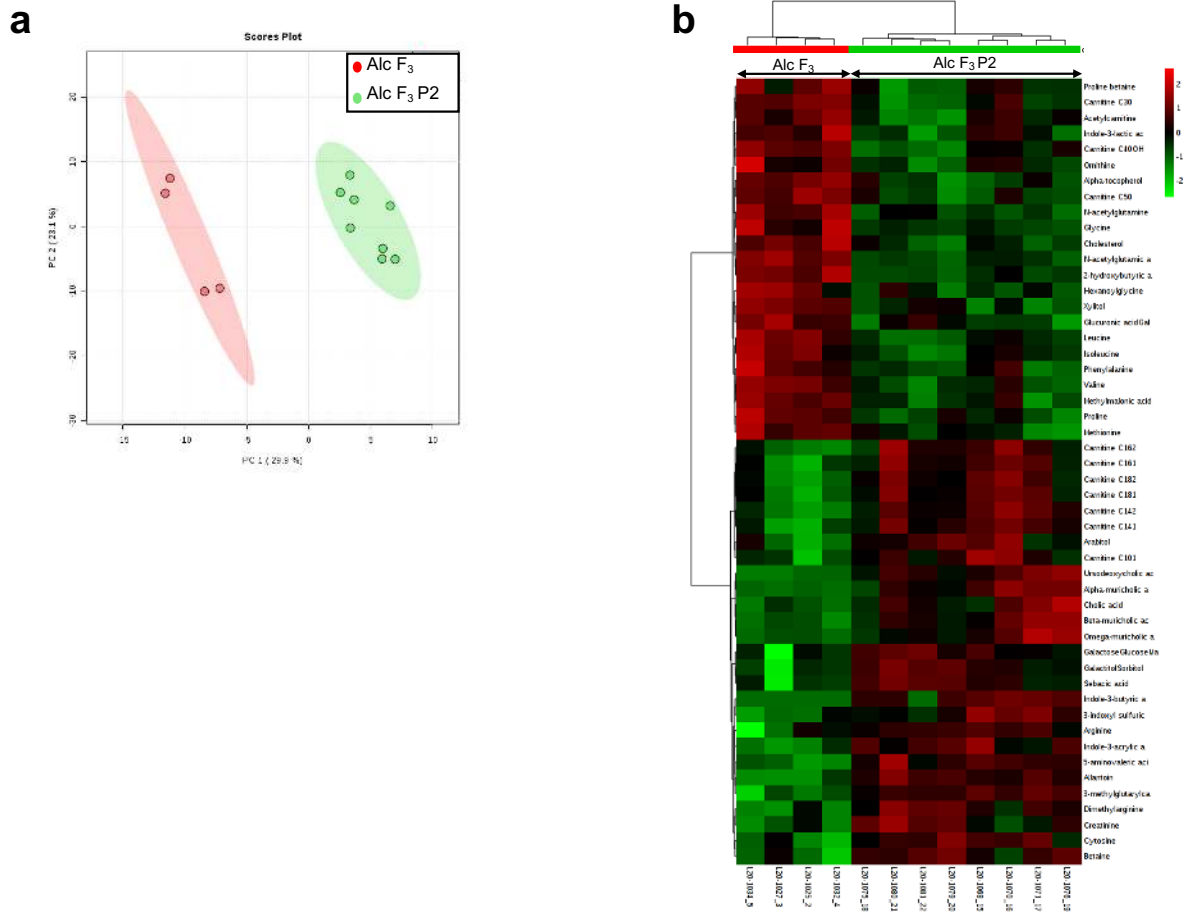
## Supplementary Figure 7



Supplementary Figure 7. Representative panels for the expression of tight junction proteins. (A) ZO-1 and (B) occludin expression in the ileum and colon.

1  
2

## Supplementary Figure 8



**Supplementary Figure 8. The fecal metabolomic profile in mice humanized with intestinal microbiota from a patient with severe alcoholic hepatitis is modified by pectin.** Alc F3 (n=4), alcohol-fed mice humanized with the microbiota from a patient with sAH (patient F3), Alc F3 P2 (n=8), alcohol-fed mice humanized with the microbiota from a patient with sAH (patient F3) and treated with 2% pectin. **(a)** PCA ordination plot of all fecal metabolomic data. **(b)** Heatmap showing the first 60 metabolites ranked by t-tests between Alc F3 (red) and Alc F3 P2 (green).

1  
2

1 **Supplementary table 1:** Clinical characteristics of donor patients with severe alcoholic  
 2 hepatitis.

<b>Patient</b>	<b>F<sub>1</sub></b>	<b>F<sub>2</sub></b>	<b>F<sub>3</sub></b>
Age (yr)	35	52	41
Alcohol consumption (g/d)	120	160	90
Duration of alcohol intake (yr)	16	20	18
BMI (kg/m <sup>2</sup> )	29	21	23
AST (IU/L)	193	153	434
Albumin (g/L)	23	27	21
Blood glucose (mmol/L)		5	5.6
Triglycerides (g/L)		0.81	1.37
PT (%)	25	30	26
Bilirubin (μmol/L)	569	92	220
Maddrey discriminant function	101	64	80
MELD	34	25	26

BMI: body mass index; AST: aspartate aminotransferase; PT: prothrombin time as percentage of control

3

4

**Supplementary table 2:** Predicted metabolomic pathways changes in intestinal microbiota

Picrust predicted metabolic pathways	Pathway	Alc F1 vs Alc F1 P6.5			Alc F2 vs Alc F2 P6.5			Alc F3 vs Alc F3 P6.5		
		Increased in	LDA	p	Increased in	LDA	p	Increased in	LDA	p
Metabolism of Cofactors and Vitamins	One carbon pool by folate	AlcF1	2.55	0.00	AlcF2	2.48	0.00	AlcF3	2.78	0.00
	Metabolism of cofactors and vitamins							AlcF3P6.5	2.41	0.00
	Ubiquinone and other terpenoid_quinone biosynthesis	AlcF1P6.5	2.35	0.00	AlcF2P6.5	2.33	0.00	AlcF3P6.5	2.52	0.00
	Thiamine metabolism	AlcF1	2.13	0.04	AlcF2	2.08	0.00	AlcF3	2.29	0.00
	Retinol metabolism				AlcF2P6.5	2.06	0.00	AlcF3P6.5	2.20	0.00
	Riboflavin metabolism							AlcF3P6.5	2.31	0.00
	Folate biosynthesis							AlcF3	2.09	0.05
	Nicotinate and nicotinamide metabolism							AlcF3	2.06	0.05
Pantothenate and CoA biosynthesis	AlcF1	2.29	0.00	AlcF2	2.37	0.00	AlcF3	2.45	0.00	
Amino Acid Metabolism	Phenylalanine metabolism	AlcF1P6.5	2.19	0.00	AlcF2P6.5	2.32	0.00	AlcF3P6.5	2.66	0.00
	Lysine biosynthesis	AlcF1	2.56	0.00	AlcF2	2.57	0.00	AlcF3	2.69	0.00
	Valine_leucine and isoleucine biosynthesis	AlcF1P6.5	2.10	0.00	AlcF2P6.5	2.33	0.00	AlcF3	2.47	0.00
	Valine_leucine and isoleucine degradation	AlcF1	2.28	0.01	AlcF2	2.37	0.00	AlcF3P6.5	2.20	0.00
	Phenylalanine_tyrosine and tryptophan biosynthesis	AlcF1	2.46	0.01	AlcF2	2.39	0.00	AlcF3	2.62	0.00
	Aminoacidrelated enzymes	AlcF1	2.79	0.00	AlcF2	2.76	0.00	AlcF3	2.98	0.00
	Lysine degradation	AlcF1P6.5	2.31	0.01	AlcF2P6.5	2.21	0.00	AlcF3P6.5	2.37	0.01
	Tyrosine metabolism	AlcF1P6.5	2.07	0.01	AlcF2P6.5	2.11	0.00	AlcF3P6.5	2.28	0.01
	Cysteine and methionine metabolism				AlcF2	2.20	0.00	AlcF3	2.20	0.00
	Histidine metabolism							AlcF3	2.70	0.00
	Tryptophan metabolism							AlcF3P6.5	2.18	0.05
	Phenylpropanoid biosynthesis							AlcF3	2.43	0.00
	Other Amino Acids	Glutathione metabolism	AlcF1P6.5	2.42	0.00	AlcF2P6.5	2.48	0.00	AlcF3P6.5	2.61
Cyanoaminoacid metabolism		AlcF1P6.5	2.12	0.02				AlcF3	2.46	0.00
D_Alanine metabolism								AlcF3	2.07	0.00
	Methane metabolism	AlcF1	2.64	0.01	AlcF2	2.62	0.00	AlcF3	2.76	0.00
	Sulfur metabolism	AlcF1P6.5	2.03	0.00	AlcF2P6.5	2.06	0.00	AlcF3P6.5	2.36	0.00



	Nitrogen metabolism	AlcF1P6.5	2.49	0.00	AlcF2P6.5	2.66	0.00	AlcF3P6.5	2.84	0.00
	Photosynthesis proteins	AlcF1	2.28	0.00	AlcF2	2.16	0.00	AlcF3	2.45	0.00
	Photosynthesis	AlcF1	2.29	0.00	AlcF2	2.16	0.00	AlcF3	2.46	0.00
	Oxidative phosphorylation							AlcF3	2.67	0.01
<b>Glycan biosynthesis and Metabolism</b>	Glycosyl transferases	AlcF1P6.5	2.31	0.01	AlcF2P6.5	2.42	0.00	AlcF3P6.5	2.52	0.00
	Lipopolysaccharide biosynthesis proteins	AlcF1P6.5	2.42	0.03	AlcF2P6.5	2.50	0.01	AlcF3P6.5	2.81	0.00
	Peptidoglycan biosynthesis	AlcF1	2.60	0.00	AlcF2	2.60	0.00	AlcF3	2.83	0.00
	Glycosaminoglyc and degradation	AlcF1P6.5	2.29	0.03	AlcF2P6.5	2.55	0.00			
	Otherglyc and degradation				AlcF2P6.5	2.87	0.00			
	Glycosphingolipid biosynthesis_ganglioseries				AlcF2P6.5	2.35	0.00			
	Lipopolysaccharide biosynthesis				AlcF2P6.5	2.28	0.01			
<b>Biosynthesis of Other Secondary Metabolites</b>	Penicillin andcephalosporin biosynthesis				AlcF2P6.5	2.03	0.00	AlcF3P6.5	2.08	0.00
	Biosynthesis andbio degradation of secondary metabolites	AlcF1P6.5	2.20	0.00						
	Butirosin and neomycin biosynthesis							AlcF3	2.22	0.00
<b>Enzyme Families</b>	Proteinkinases	AlcF1P6.5	2.27	0.05				AlcF3P6.5	2.50	0.00
	Peptidases	AlcF1	2.68	0.00	AlcF2	2.51	0.01	AlcF3	2.79	0.00
<b>Carbohydrate Metabolism</b>	Galactose metabolism	AlcF1P6.5	2.65	0.00	AlcF2P6.5	2.78	0.00	AlcF3P6.5	2.53	0.05
	Glyoxylate and dicarboxylate metabolism	AlcF1P6.5	2.35	0.00	AlcF2P6.5	2.45	0.00	AlcF3P6.5	2.80	0.00
	Fructose and mannose metabolism	AlcF1P6.5	2.40	0.02	AlcF2P6.5	2.63	0.00	AlcF3P6.5	2.85	0.00
	Starch and sucrose metabolism	AlcF1P6.5	2.66	0.00	AlcF2P6.5	2.41	0.00	AlcF3	2.40	0.01
	Pentose and glucuronate interconversions	AlcF1P6.5	2.70	0.00	AlcF2P6.5	2.79	0.00	AlcF3P6.5	2.96	0.00
	Ascorbate and aldarate metabolism	AlcF1P6.5	2.29	0.02	AlcF2P6.5	2.03	0.00	AlcF3P6.5	2.51	0.01
	Pyruvate metabolism				AlcF2P6.5	2.12	0.01	AlcF3P6.5	2.51	0.00
	Propanoate metabolism				AlcF2P6.5	2.23	0.04	AlcF3P6.5	2.60	0.00
	Pentose phosphate pathway				AlcF2P6.5	2.03	0.01	AlcF3P6.5	2.41	0.00
	Glycolysis_Gluconeogenesis							AlcF3P6.5	2.02	0.01
	Butanoate metabolism							AlcF3P6.5	2.43	0.00
	Inositolphosphate metabolism							AlcF3P6.5	2.37	0.00
	Biosynthesis and biodegradation of secondary metabolites							AlcF3P6.5	2.38	0.00
	Carbohydrate metabolism							AlcF3P6.5	2.65	0.00
	Glycan biosynthesis and metabolism							AlcF3P6.5	2.11	0.01

	Aminosugar and nucleotidesugar metabolism				AlcF2P6.5	2.51	0.00		
<b>Lipid Metabolism</b>	Fattyacid metabolism	AlcF1P6.5	2.29	0.03	AlcF2P6.5	2.33	0.00	AlcF3P6.5	2.56 0.00
	Biosynthesis of unsaturated fatty acids	AlcF1P6.5	2.18	0.01				AlcF3P6.5	2.37 0.00
	Fattyacid biosynthesis				AlcF2P6.5	2.02	0.00	AlcF3P6.5	2.19 0.03
	Glycerophospholipid metabolism				AlcF2	2.12	0.00	AlcF3	2.29 0.00
	Glycerolipid metabolism	AlcF1	2.23	0.00	AlcF2	2.31	0.00		
	Lipid biosynthesis proteins				AlcF2P6.5	2.03	0.00		
	Sphingolipid metabolism	AlcF1P6.5	2.36	0.04	AlcF2P6.5	2.58	0.00		
<b>Xenobiotics Bio degradation and Metabolism</b>	Drug metabolism_other enzymes	AlcF1	2.07	0.02	AlcF2	2.05	0.01	AlcF3	2.45 0.00
	Drug metabolism_cytochrome P450	AlcF1P6.5	2.01	0.00	AlcF2P6.5	2.10	0.00	AlcF3P6.5	2.21 0.00
	Metabolism of xenobiotics by cytochrome P450	AlcF1P6.5	2.02	0.00	AlcF2P6.5	2.08	0.00	AlcF3P6.5	2.21 0.00
	Benzoate degradation				AlcF2P6.5	2.06	0.04	AlcF3P6.5	2.50 0.00
	Caprolactam degradation	AlcF1P6.5	2.07	0.04				AlcF3P6.5	2.27 0.00
	Naphthalene degradation				AlcF2P6.5	2.03	0.00		
	Dioxin degradation							AlcF3P6.5	2.28 0.00
	Xylene degradation							AlcF3P6.5	2.20 0.00
	Toluene degradation							AlcF3P6.5	2.25 0.00
<b>Nucleotide Metabolism</b>	Pyrimidine metabolism	AlcF1	2.98	0.00	AlcF2	2.93	0.00	AlcF3	3.16 0.00
	Purine metabolism	AlcF1	2.78	0.00	AlcF2	2.65	0.00	AlcF3	2.85 0.01
<b>Metabolism of Terpenoids and Polyketides</b>	Prenyl transferases	AlcF1	2.20	0.01	AlcF2	2.15	0.01	AlcF3	2.43 0.00
	Terpenoid backbone biosynthesis	AlcF1	2.52	0.00	AlcF2	2.44	0.00	AlcF3	2.64 0.00
	Geraniol degradation	AlcF1P6.5	2.22	0.00	AlcF2P6.5	2.24	0.00	AlcF3P6.5	2.40 0.00
	Biosynthesis of siderophore group nonribosomal peptides	AlcF1P6.5	2.17	0.00	AlcF2P6.5	2.02	0.00	AlcF3P6.5	2.46 0.00
	Tetracycline biosynthesis							AlcF3P6.5	2.14 0.00

**Supplementary table 3:** Pathways modified in pectin treated mice based on fecal metabolomic analysis

Pathway Name	Nb of compounds included in the analysis	Total compounds in pathway	p	FDR	Impact
Inositol phosphate metabolism	2	28	0.000	0.000	0.11163
Ascorbate and aldarate metabolism	3	9	0.000	0.000	0.4
Starch and sucrose metabolism	5	19	0.000	0.000	0.24448
Methane metabolism	2	9	0.000	0.000	0.4
Cyanoamino acid metabolism	2	6	0.000	0.000	0
Lysine biosynthesis	1	4	0.000	0.000	0
Lysine degradation	1	23	0.000	0.000	0
Biotin metabolism	1	5	0.000	0.000	0
Purine metabolism	13	68	0.000	0.000	0.14028
Tyrosine metabolism	3	44	0.000	0.000	0.14045
Valine, leucine and isoleucine degradation	5	38	0.000	0.000	0.0238
Porphyrin and chlorophyll metabolism	2	27	0.000	0.000	0
Pentose and glucuronate interconversions	5	16	0.000	0.000	0.26666
Valine, leucine and isoleucine biosynthesis	6	11	0.000	0.000	0.99999
Histidine metabolism	3	15	0.000	0.000	0.24194
Glyoxylate and dicarboxylate metabolism	2	18	0.000	0.000	0.32258
Citrate cycle (TCA cycle)	5	20	0.000	0.000	0.24593
D-Glutamine and D-glutamate metabolism	3	5	0.000	0.000	1
Nitrogen metabolism	4	9	0.000	0.000	0
Linoleic acid metabolism	1	16	0.000	0.000	1
Pantothenate and CoA biosynthesis	5	15	0.000	0.001	0.02041
Cysteine and methionine metabolism	4	27	0.000	0.001	0.1351
Aminoacyl-tRNA biosynthesis	18	69	0.000	0.001	0.12903
Glutathione metabolism	6	26	0.000	0.001	0.09828
beta-Alanine metabolism	4	17	0.000	0.001	0.44444
Butanoate metabolism	6	22	0.000	0.001	0.02899

Alanine, aspartate and glutamate metabolism	10	24	0.000	0.001	0.78269
Glycine, serine and threonine metabolism	10	31	0.000	0.001	0.59903
Ubiquinone and other terpenoid-quinone biosynthesis	1	3	0.001	0.001	0
Primary bile acid biosynthesis	5	46	0.001	0.001	0.12626
Sphingolipid metabolism	2	21	0.001	0.001	0.01504
Phenylalanine, tyrosine and tryptophan biosynthesis	2	4	0.001	0.002	1
Phenylalanine metabolism	2	11	0.001	0.002	0.40741
Steroid biosynthesis	1	35	0.002	0.002	0.05394
Steroid hormone biosynthesis	1	72	0.002	0.002	0.01689
Pyrimidine metabolism	5	41	0.002	0.003	0.08292
Galactose metabolism	6	26	0.002	0.003	0.07627
Arginine and proline metabolism	14	44	0.003	0.004	0.54477
Taurine and hypotaurine metabolism	3	8	0.003	0.004	0.71428
Selenoamino acid metabolism	1	15	0.004	0.005	0
Pyruvate metabolism	2	23	0.004	0.006	0.18375
Propanoate metabolism	2	20	0.006	0.007	0
Fatty acid elongation in mitochondria	1	27	0.008	0.010	0
Fatty acid metabolism	1	39	0.008	0.010	0
Glycerolipid metabolism	3	18	0.010	0.013	0.41129
Pentose phosphate pathway	4	19	0.018	0.021	0.41291
Glycolysis or Gluconeogenesis	3	26	0.018	0.021	0.13406
Biosynthesis of unsaturated fatty acids	7	42	0.020	0.023	0
Nicotinate and nicotinamide metabolism	2	13	0.034	0.038	0.2381
Fatty acid biosynthesis	4	43	0.035	0.038	0
Tryptophan metabolism	2	40	0.041	0.044	0.28702
Glycerophospholipid metabolism	5	30	0.046	0.048	0.11297
Amino sugar and nucleotide sugar metabolism	2	37	0.144	0.147	0.08988
Arachidonic acid metabolism	1	36	0.384	0.384	0.32601

FDR: false discovery rate

1 **Supplementary table 4:** Clinical characteristics of alcoholic patients for tryptophan pathway  
 2 analysis.

	<b>Alcoholic patients without alcoholic hepatitis (noAH) (n=15)</b>	<b>Alcoholic patients with severe alcoholic hepatitis (sAH) (n=14)</b>
Age (years)	52.07 ± 8.21	55.79 ± 12.4
Sex (male,%)	10 (67)	13 (93)
BMI (kg/m <sup>2</sup> )	22.08 ± 4.3	25.56 ± 5.05
Alcohol (g/day)*	149.14 ± 101.81	77.86 ± 36.2
Alcohol duration (years)	15.04 ± 12.31	21.23 ± 10.37
Smoking (yes,%)	11 (73)	9 (64)
AST (IU/L)**	38.93 ± 20.83	131.36 ± 105.03
ALT (IU/L)	36.27 ± 16.18	42.5 ± 16.58
Bilirubin**	13.13 ± 7.72	229 ± 221.84
GGT (IU/L)*	121.73 ± 97.53	423.43 ± 384.51
Platelets (×10 <sup>9</sup> /L) *	211.93 ± 72.48	127 ± 114.12
PT (%)***	98.67 ± 4.13	39 ± 14.46
MELD score***	2.78 ± 2.92	22.84 ± 7.5

BMI: body mass index, AST: aspartate transaminase, ALT: alanine transaminase, GGT: gamma-glutamyltransferase, PT: prothrombin time, MELD: Model for End-Stage Liver Disease. \*<0.05, \*\*<0.01, \*\*\*<0.001. Data are presented as mean ± SD.

3

4

1 **Supplementary table 5:** Primer sequences used for q-PCR reactions

Name	5'- Forward - 3'	5'- Reverse - 3'
<i>18s</i>	GTAACCCGTTGAACCCATT	CCATCCAATCGGTAGTAGCG
<i>ahrr</i>	ACATACGCCGGTAGGAAGAGA	GGTCCAGCTCTGTATTGAGGC
<i>ccl2</i>	AGGTCCCTGTCATGCTTCTG	TCTGGACCCATTCCCTTCTTG
<i>ccl3</i>	<i>purchased from Qiagen , ref QT00248199</i>	
<i>cyp1a1</i>	CAGGATGTGTCTGGTTACTTTGAC	CTGGGCTACACAAGACTCTGTCTC
<i>gapdh</i>	GTGGACCTCATGGCCTACAT	TGTGAGGGAGATGCTCAGTG
<i>il1β</i>	AAGGTCCACGGGAAAGACAC	AGCTTCAGGCAGGCAGTATC
<i>il17</i>	TTTAACTCCCTTGCGCAAAA	CTTCCCTCCGCATTGACAC
<i>il22</i>	ATGAGTTTTTCCCTTATGGGGAC	GCTGGAAGTTGGACACCTCAA
<i>reg3β</i>	GGCAACTTCACCTCACAT	TGGGAATGGAGTAACAATG
<i>reg3γ</i>	CAAGATGTCCTGAGGGC	CCATCTTCACGTAGCAGC
<i>scd1</i>	CCGGAGACCCTTAGATCGA	TAGCCTGTAAAAGATTTCTGCAAA
<i>tgfβ</i>	GCAACATGTGGA ACTCTACCAGAA	GACGTCAAAAGACAGCCACTCA
<i>tnfa</i>	TGGGAGTAGACAAGGTACAACCC	CATCTTCTCAA AATTCGAGTGACAA

2

3

4